

Status report of the DIRAC experiment (PS 212)

L.Nemenov

SPS Committee, April 3, 2012.

DIRAC collaboration



CERN

Geneva, Switzerland



Czech Technical University

Prague, Czech Republic



Institute of Physics ASCR

Prague, Czech Republic



Nuclear Physics Institute ASCR

Rez, Czech Republic



INFN-Laboratori Nazionali di Frascati

Frascati, Italy



University of Messina

Messina, Italy



KEK

Tsukuba, Japan



Kyoto University

Kyoto, Japan



Kyoto Sangyou University

Kyoto, Japan



Tokyo Metropolitan University

Tokyo, Japan



IFIN-HH

Bucharest, Romania



JINR

Dubna, Russia



SINP of Moscow State University

Moscow, Russia



IHEP

Protvino, Russia



Santiago de Compostela University

Santiago de Compostela, Spain



Bern University

Bern, Switzerland



Zurich University

Zurich, Switzerland

Content

- 1. Long-lived $\pi^+\pi^-$ atoms : data taking in 2011 for their observation and data processing schedule in 2012.**
- 2. Status of the run 2012 preparation for the long-lived $\pi^+\pi^-$ atom observation.**
- 3. Status and schedule of data (2008-10) analysis of $K^+\pi^-$, $K^-\pi^+$ and $\pi^+\pi^-$ atoms in 2012.**
- 4. Multiple-scattering measurement during 2011 run and data processing schedule.**
- 5. Published results of $\pi^+\pi^-$ atom lifetime measurement.**

DIRAC setup

Upgraded DIRAC setup

single and multilayer targets

P
vacuum

MDC
shield1

SFD
IH
shield2

vacuum

magnet

π^+, p, K^+
 π^-, \tilde{p}, K^-

MDC, 18 planes

SFD

IH

heavy gas
Cherenkov
aerogel

DC
VH
HH

Ch
PSh
Mu

π^+, K^+, p

T1

absorber

1 meter

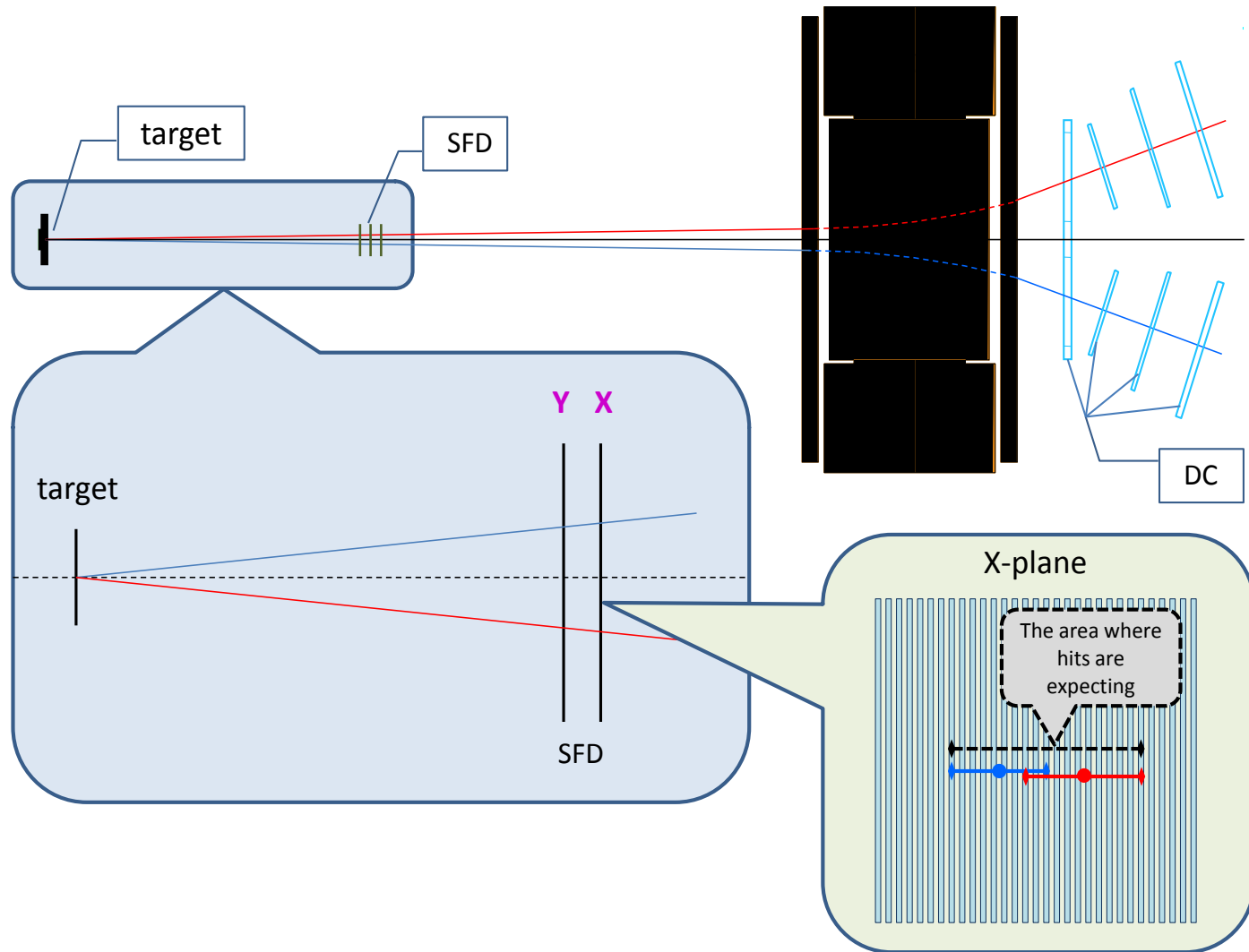
π^-, K^-, \tilde{p}

T2

Modified parts

MDC - microdrift gas chambers, SFD - scintillating fiber detector, IH – ionization hodoscope. DC - drift chambers , VH – vertical hodoscopes, HH – horizontal hodoscopes, Ch – nitrogen Cherenkov , PSh - preshower detectors , Mu - muon detectors

Extrapolation to the target

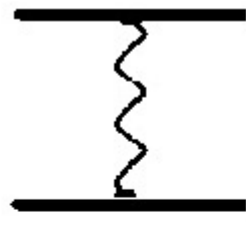


ENERGY SPLITTING MEASUREMENT

$A_{2\pi}$ Energy Levels

J. Schweizer [PL B (2004)]

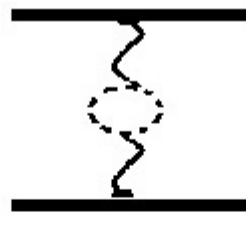
For Coulomb potential
E depends on n only.



2s 2p

ns np; nl, l>1

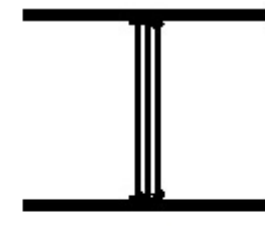
Coulomb potential



2s 2p

ns np; nl, l>1

Vacuum polarisation



2p

2s

ns np; nl, l>1

Strong potential

$$E_{2s} - E_{2p} = \Delta_{2s-2p} \quad \Delta_{2s-2p}^{\text{vac}} = -0.107 \text{ eV} \quad \Delta_{2s-2p}^{\text{str}} = -0.47 \text{ eV}$$

$$\Delta_{2s-2p}^{\text{vac+str}} = -0.58 \text{ eV}$$

$$\Delta_{2s-2p}^{\text{tot}} = -0.59 \pm 0.01 \text{ eV}$$

$$\Delta_{2s-2p}^{\text{str}} = -\frac{\alpha^3 m_\pi}{8} \frac{1}{6} (2a_0 + a_2) + \dots$$

$$\Delta_{\text{ns-np}} = -\frac{\Delta_{2s-2p}}{n^3} \cdot 8$$

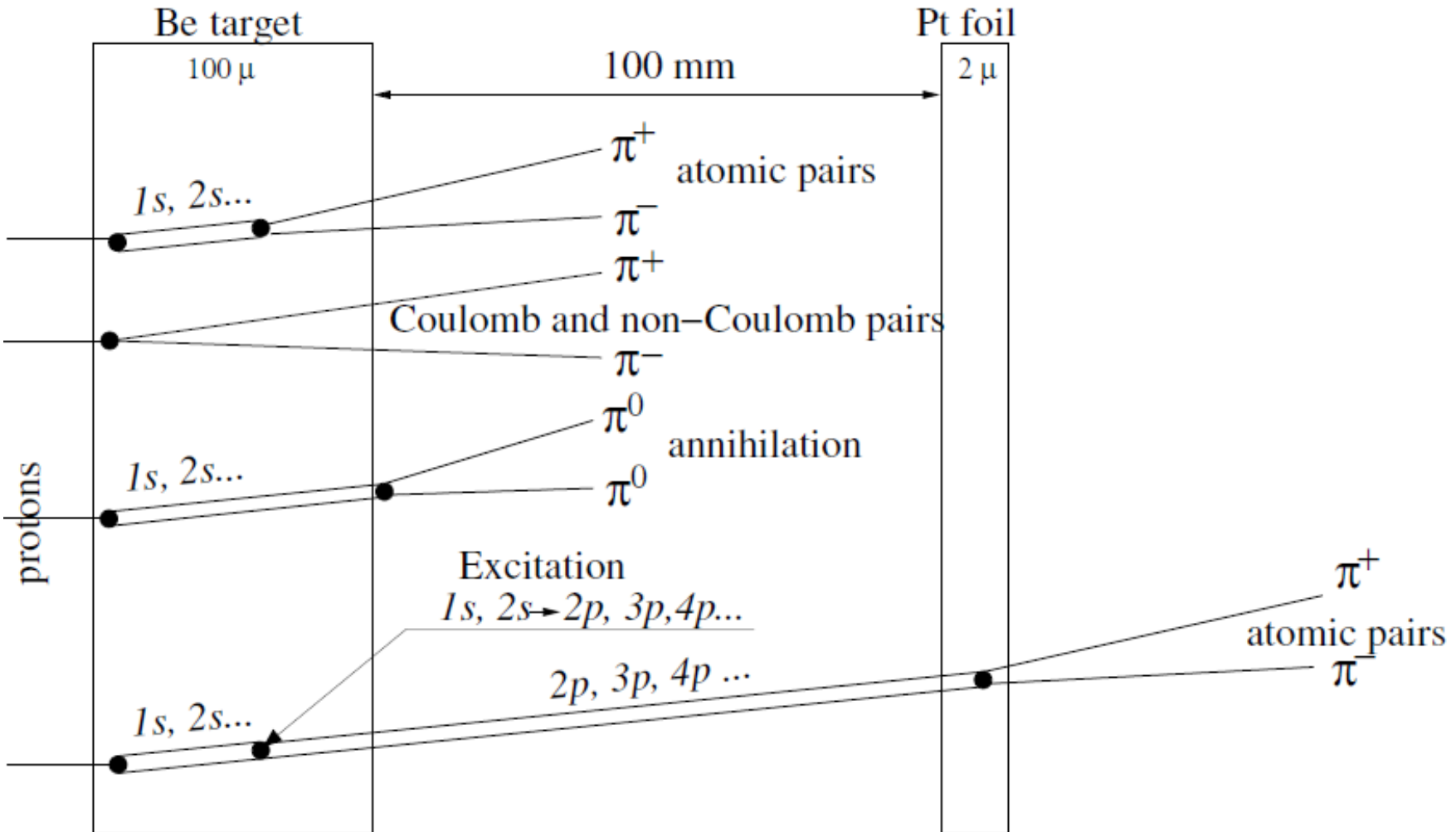
CONCLUSION: one parameter ($2a_0 + a_2$) allows to calculate all $\Delta_{\text{ns-np}}$ values.

Long-lived $\pi^+\pi^-$ atoms

The observation of $\pi\pi$ atom long-lived states opens the future possibility to measure the energy difference between ns and np states $\Delta E(ns-np)$ and the value of $\pi\pi$ scattering lengths $|2a_0+a_2|$.

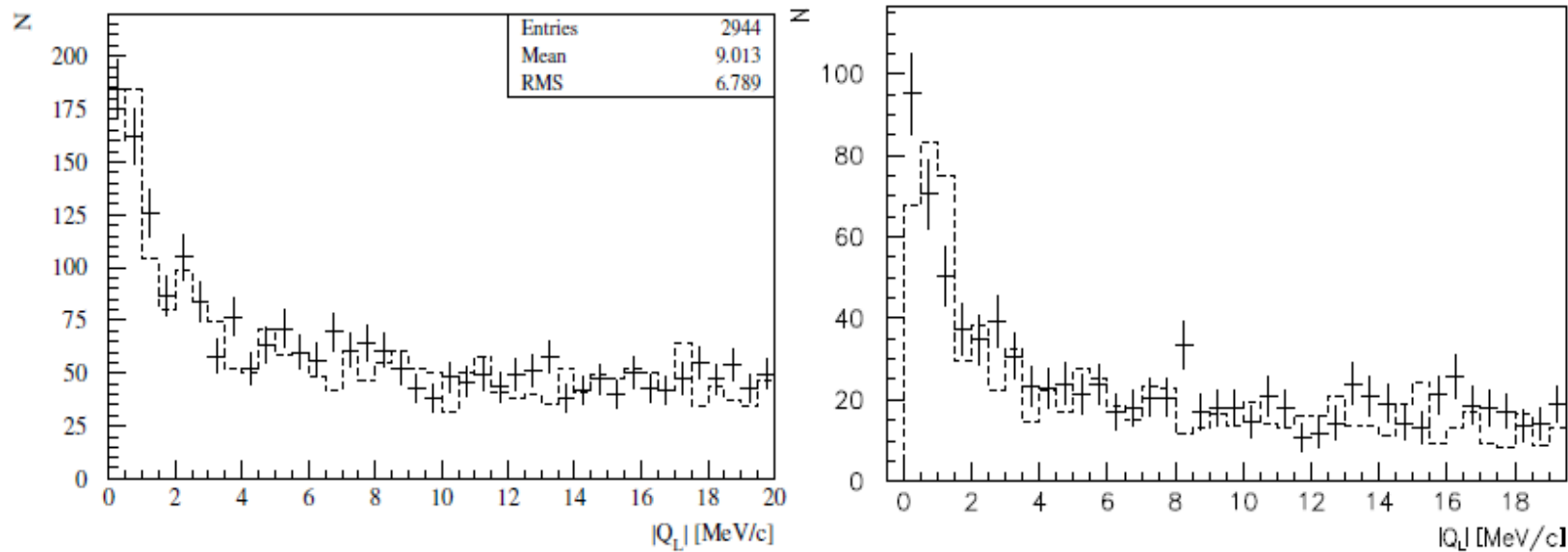
If a resonance method can be applied for the $\Delta E(ns-np)$ measurement, then the precision of $\pi\pi$ scattering length measurement can be improved by one order of magnitude relative to the precision of other methods.

Method to observe long-lived $A_{2\pi}$ by means of a breakup foil of Platinum



Production of $A_{2\pi}$ in Beryllium target

Distribution over $|Q_L|$ of $\pi^+\pi^-$ pairs collected in 2010 (left) and in 2011 (right) with Beryllium target with the cut $Q_T < 1$ MeV/c. Experimental data (points with error bars) have been fitted by a sum of the simulated distribution of “Coulomb” and “non-Coulomb” pairs (dashed line).



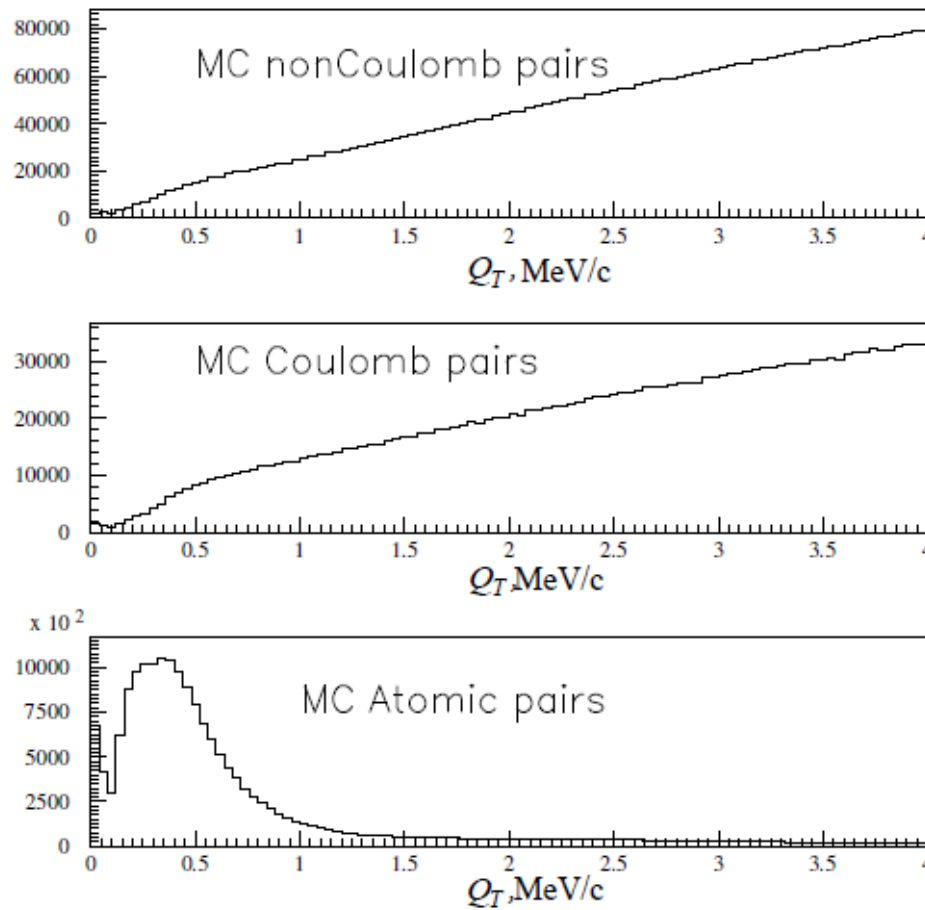
Produced atom numbers normalized on the proton flux:

$$N_{A_{2\pi}}/p = (5.1 \pm 0.5) \times 10^{-14} \text{ (2010)}$$

$$N_{A_{2\pi}}/p = (5.9 \pm 0.5) \times 10^{-14} \text{ (2011)}$$

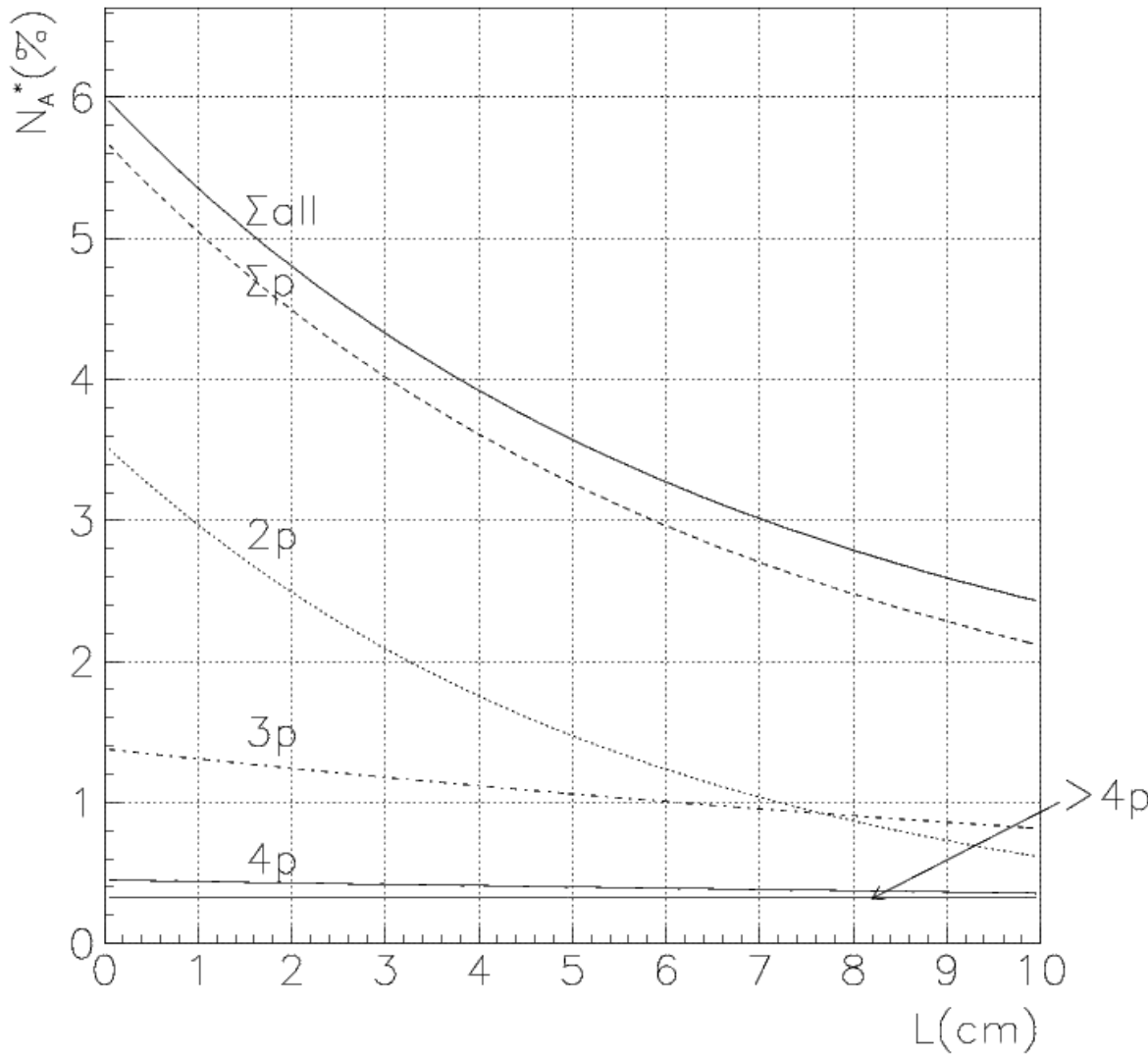
Simulation of $\pi^+\pi^-$ pairs from Beryllium target and "atomic pairs" from Platinum foil

Distributions of reconstructed values of Q_T for non-Coulomb, Coulomb pairs and pairs from metastable atom



“Long-lived $A_{2\pi}$ ” yield and quantum numbers

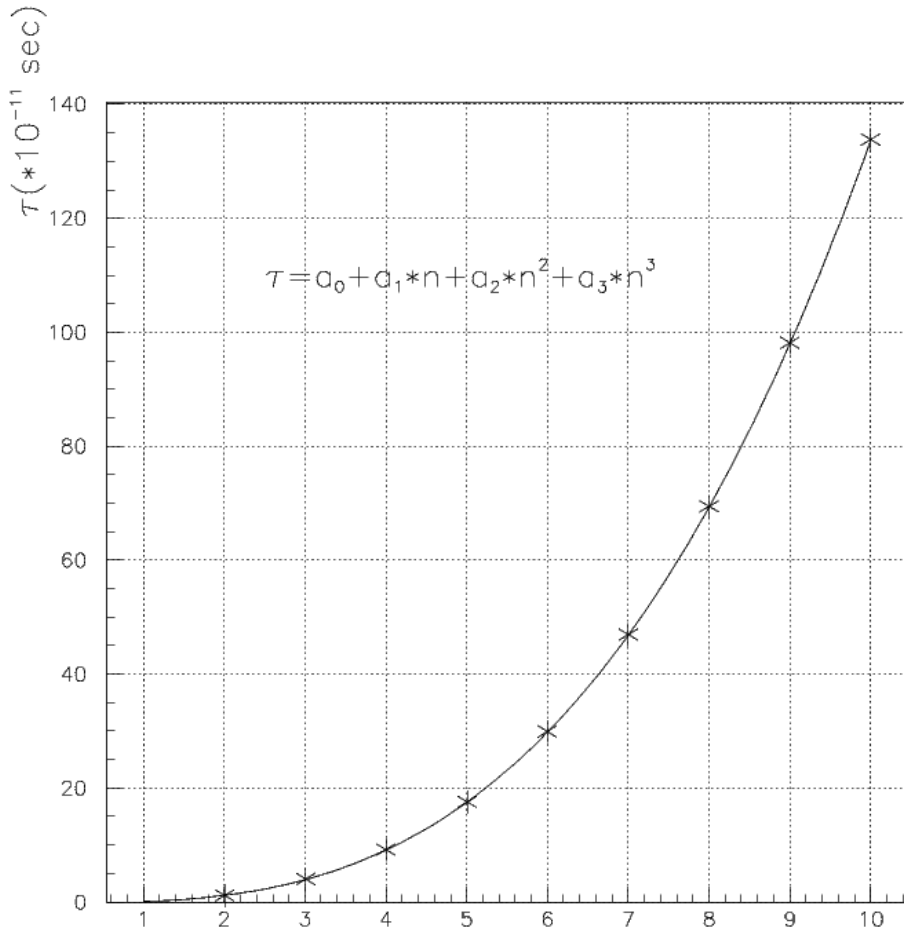
L. Afanasev; O. Gorchakov (DIPGEN)



Atomic pairs from “long-lived $A_{2\pi}$ ” breakup in $2\mu\text{m}$ Pt.

A_{2π} lifetime, τ, in np states

M. Pentia



n _H	τ _H • 10 ⁸ s	τ _{2π} • 10 ¹¹ s	Decay length A _{2π} in L.S. cm for γ=16.1
2p	0.16	1.17	5.7
3p	0.54	3.94	19
4p	1.24	9.05	44
5p	2.40	17.5	84.5
6p	4.1	29.9	144
7p		46.8*	226
8p		69.3*	335

Production, annihilation and breakup of long-lived $A_{2\pi}$

Relative populations (%) of $A_{2\pi}$ long-lived states at the Be target exit as a function of principal quantum number n and orbital momentum l

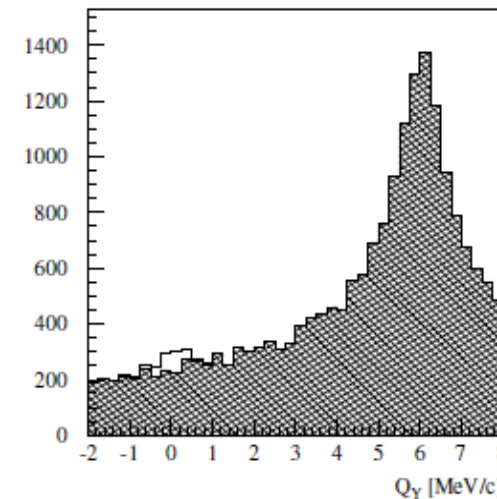
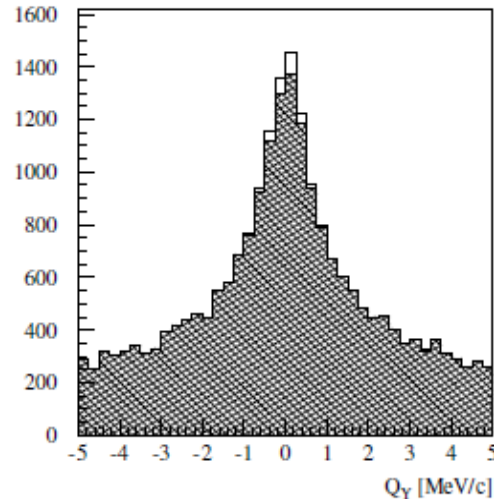
$l \backslash n$	2	3	4	5	6	7	8
1	417	148	48	18	7	3	1
2	0	117	49	20	9	4	1
3	0	0	45	21	10	4	2
4	0	0	0	20	10	5	2
5	0	0	0	0	10	5	2
6	0	0	0	0	0	4	2
7	0	0	0	0	0	0	2

Breakup probability of $A_{2\pi}$ in np states for different thicknesses of Platinum foils ($A_{2\pi}$ momentum $P_A = 4.5 \text{ GeV}/c$ and $A_{2\pi}$ ground-state lifetime $\tau = 3 \times 10^{-15} \text{ s}$)

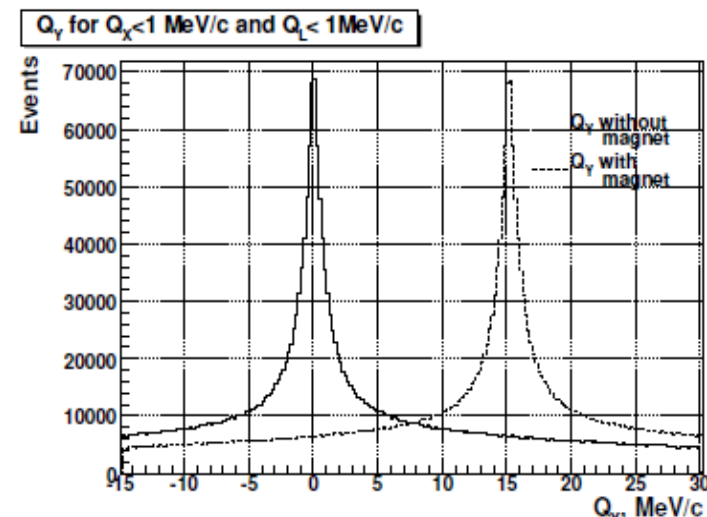
Thickness (μm)	2p	3p	4p	5p	6p	7p
0.1	0.0251	0.0520	0.0858	0.1327	0.2035	0.3219
0.2	0.0559	0.1175	0.1978	0.3001	0.4185	0.5392
0.5	0.1784	0.3595	0.5537	0.7176	0.8323	0.9043
1.0	0.4147	0.6895	0.8553	0.9324	0.9667	0.9828
1.5	0.6084	0.8526	0.9446	0.9765	0.9889	0.9944
2.0	0.7422	0.9244	0.9743	0.9895	0.9951	0.9975
3.0	0.8844	0.9739	0.9918	0.9967	0.9985	0.9992

Simulation of the permanent magnets influence

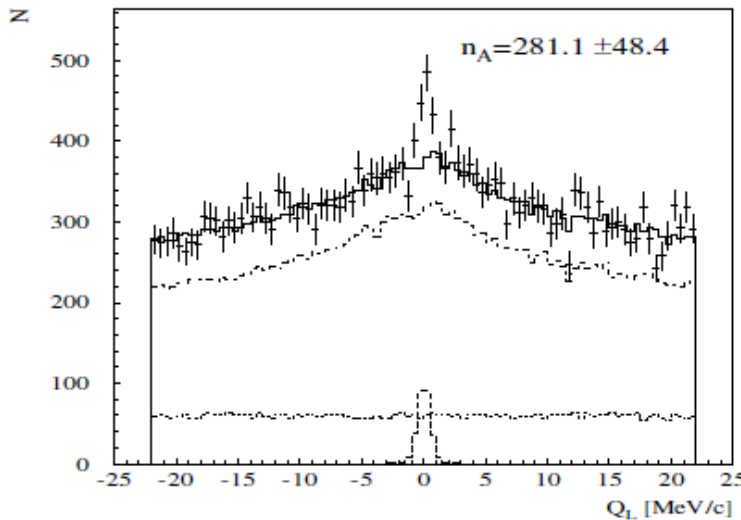
Simulated “atomic pairs” from long-lived atoms (light area) over Q_Y above the background of $\pi^+\pi^-$ pairs produced in Beryllium target with cuts $|Q_X| < 1 \text{ MeV}/c$, $|Q_L| < 1 \text{ MeV}/c$ (hatched area). In left side without the magnet and in right side with magnet used in 2011



Simulated distribution of $\pi^+\pi^-$ pairs over Q_Y produced in Beryllium target with cuts $|Q_X| < 1 \text{ MeV}/c$, $|Q_L| < 1 \text{ MeV}/c$. The events without magnet (solid line) are distributed around 0 and events with the new magnet are shifted by 15 MeV/c (dashed line)

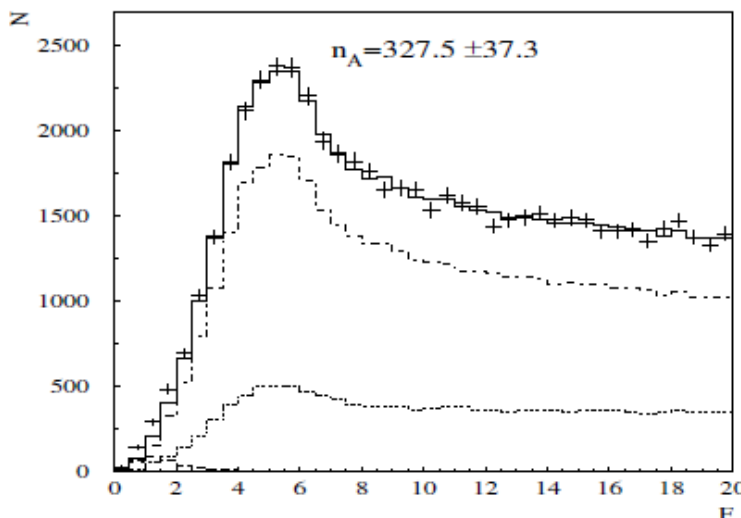


Simulation of extraction the long-lived $A_{2\pi}$ signal



Simulated distribution of $\pi^+\pi^-$ pairs over Q_L , with criterion $Q_T < 1$ MeV/c.

“Experimental data” (points with error bars) are fitted by the sum of “atomic pairs” from long-lived states (dashed line), “Coulomb pairs” (by dotted-dashed line), “non-Coulomb pairs” (dotted line). The background sum is shown by the solid line.



Simulated distribution of $\pi^+\pi^-$ pairs over F , with criterion $Q_T < 2$ MeV/c. “Experimental data” (points with error bars) are fitted by the sum of “atomic pairs” from long-lived states (dashed line), “Coulomb pairs” (dotted-dashed line), “non-Coulomb pairs” (dotted line). The background sum is shown by the solid line.

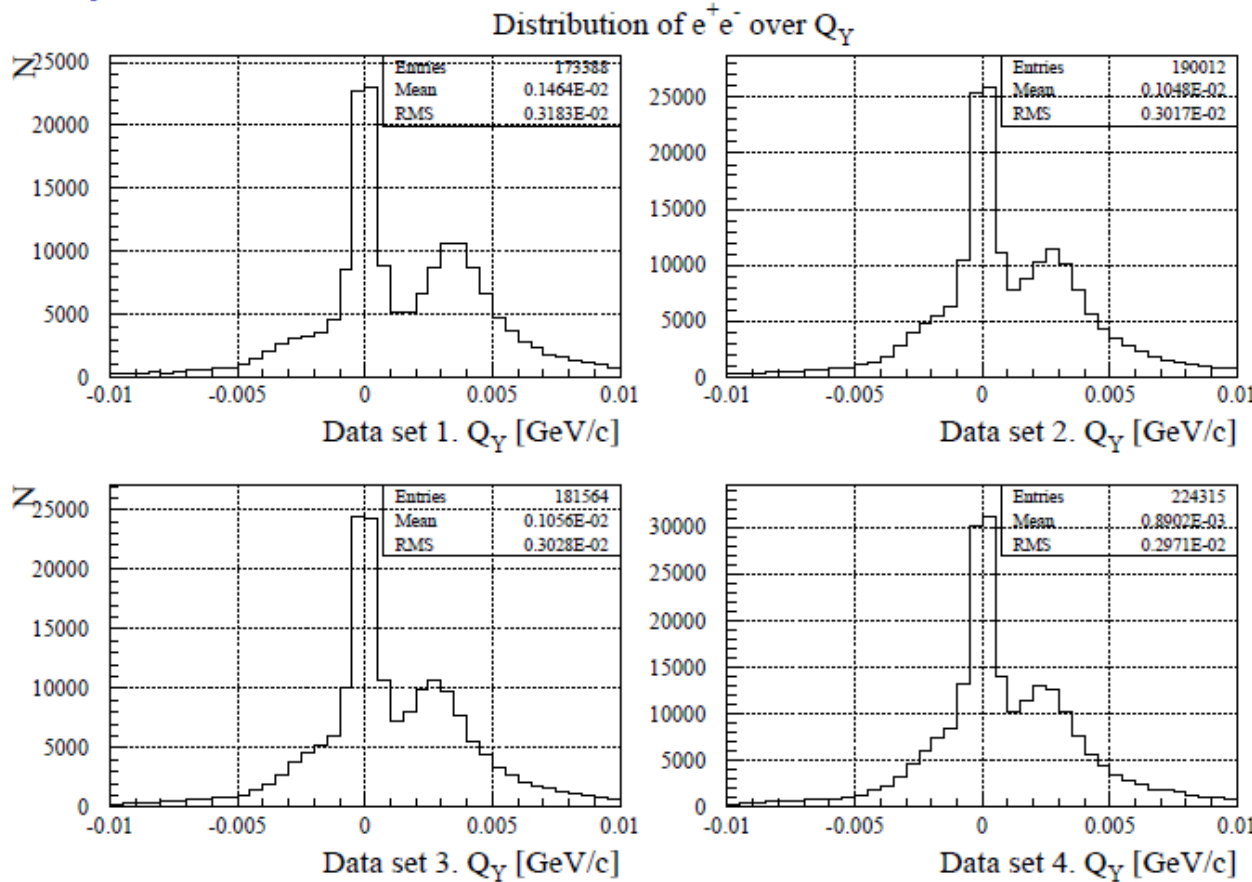
Maximal estimation of particles fluxes through the permanent magnet

Maximal estimation of π , p , n , γ flux due to nuclear interaction of 24 GeV protons with the Beryllium target

Fluxs of high energy particles	
$\pi^+ \& \pi^-$	$10^4 \text{ spill}^{-1} \text{cm}^{-2}$
p	$0.23 \cdot 10^4 \text{ spill}^{-1} \text{cm}^{-2}$
n	$0.23 \cdot 10^4 \text{ spill}^{-1} \text{cm}^{-2}$
γ	$10^4 \text{ spill}^{-1} \text{cm}^{-2}$
Total per run	$2.5 \cdot 10^{10} \text{ cm}^{-2}$

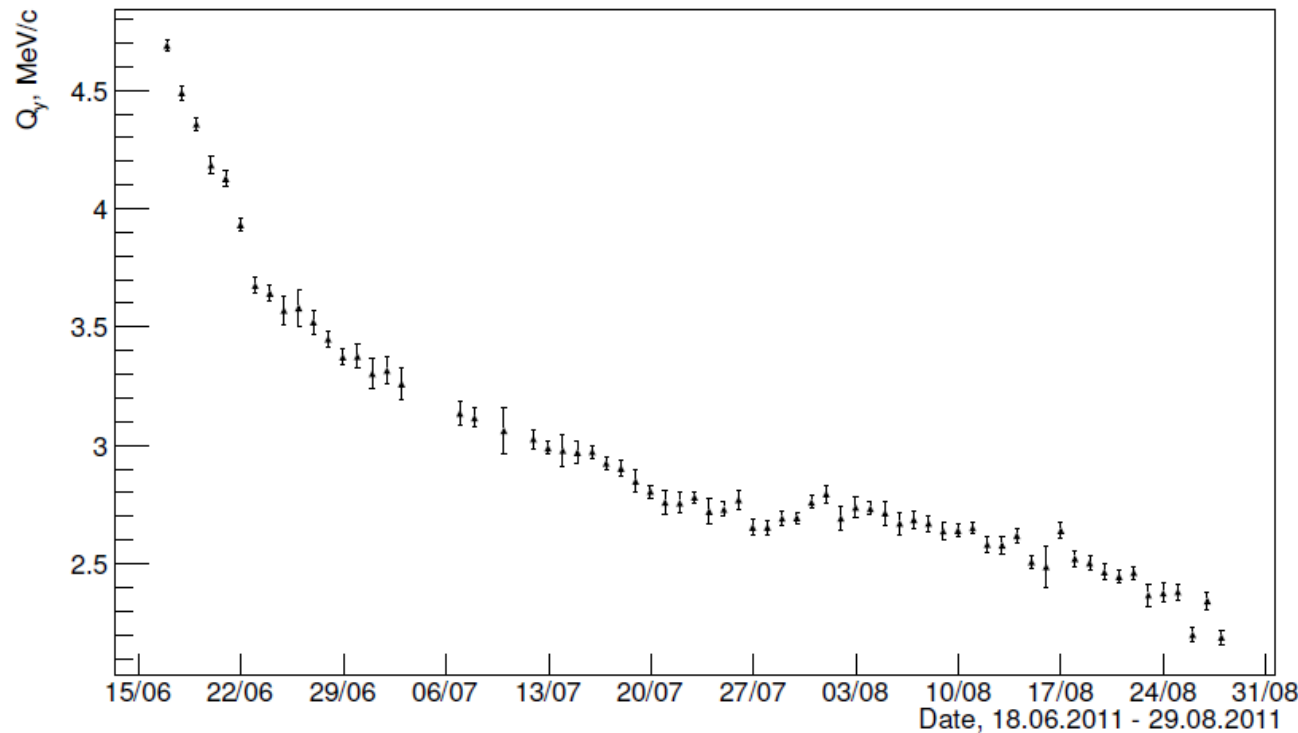
Neutron evaporation from the Be target	
Total per run	$3.2 \cdot 10^{12} \text{ cm}^{-2}$

2011 experimental e^+e^- distribution over Q_Y



e^+e^- pair distributions over Q_Y . for 4 time intervals: data set 1 — from 25/06/2011 to 01/07/2011; data set 2 — from 22/07/2011 to 31/07/2011; data set 3 — from 04/08/2011 to 09/08/2011; data set 4 — from 24/08/2011 to 28/08/2011. Changing in position of the peak at non-zero Q_Y illustrates the permanent magnet degradation.

Degradation of the permanent magnet in June - August 2011



The position of second peak in Q_y distributions of e^+e^- pairs versus dates.

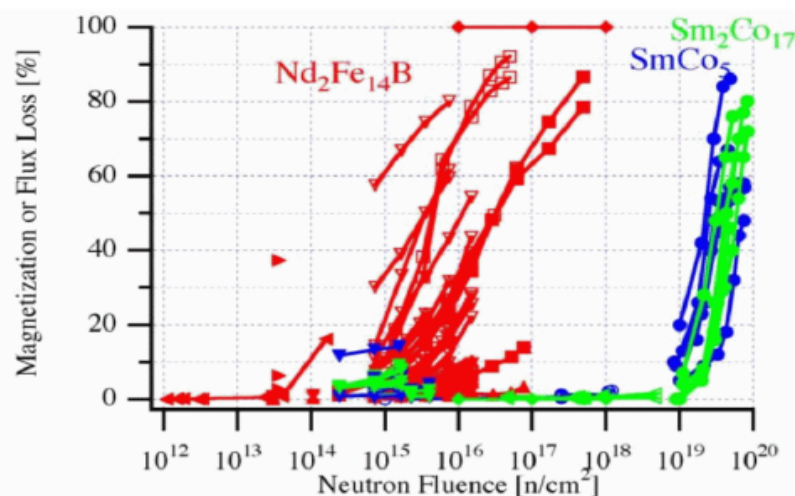
Plan of 2011 run data processing

- End of data preselection : June 2012
- Ntuple preparation completion : August 2012
- Atomic pair signal from “long-lived atom” ionization without magnetic field is expected on the level of about 3.5 sigma.

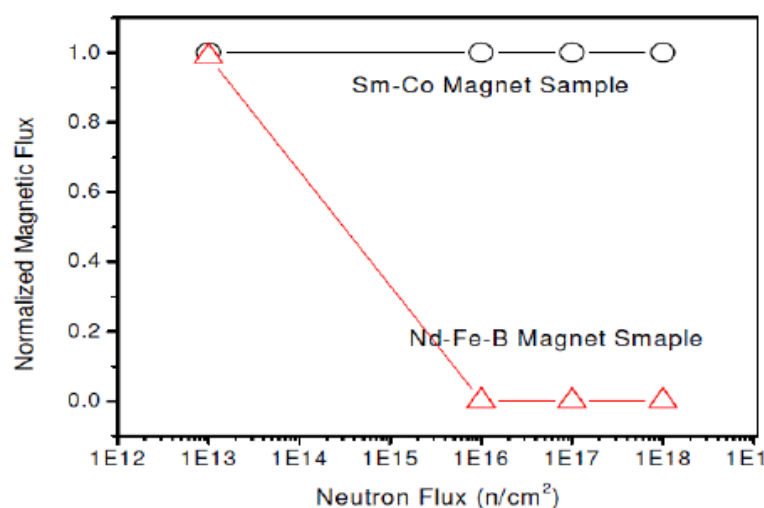
Magnet for 2012 run

- 2 new magnets:
 $\text{Sm}_2\text{Co}_{17}$, high resistivity against radiation,
 $BL = 0.02 \text{ Tm}$, expected signal > 9 sigma.
- New retracting device allows to replace magnet fast.
- Magnet will be ready in the middle of April.
- Retracting device will be ready at the end April.

Magnetization loss of various permanent magnet because of neutron irradiations

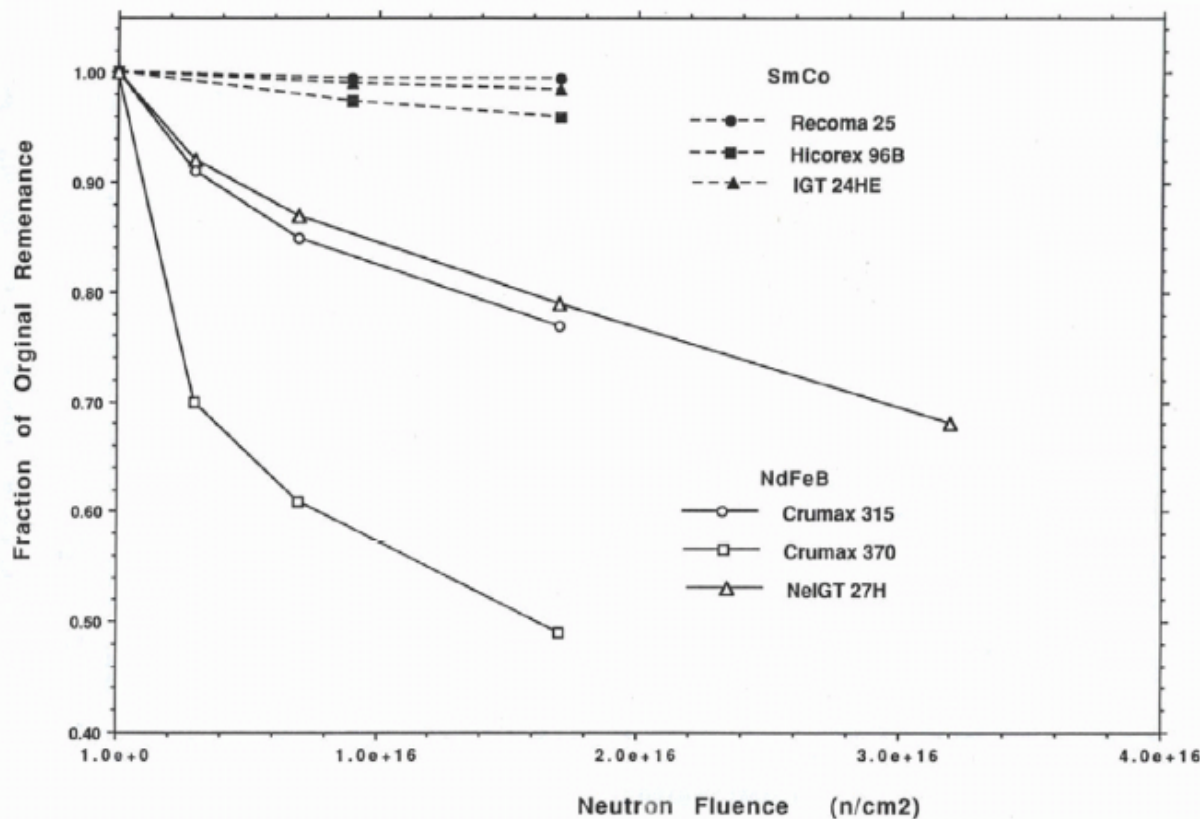


Summary on the magnetization loss in % versus the neutron fluxes per cm² for Nd-Fe-B and Sm-Co magnets. The Nd-Fe-B magnets (red lines) have been irradiated by 65 MeV neutrons. The Sm-Co magnets (blue and green lines) have been irradiated by spallation sources with a high energy tail but a peak at low energy (1~15 MeV).



Normalized magnetization of Nd-Fe-B and Sm-Co magnets versus the reactor neutron flux.

Magnetization loss of various permanent magnet because of proton irradiations



Normalized magnetization of Nd-Fe-B and Sm-Co magnets versus fluxes of the neutron produced by a high-intensity proton beam of 86 MeV.

Permanent dipole magnet for DIRAC

Permanent magnet material: Sm₂Co₁₇

Alexey Vorozhtsov

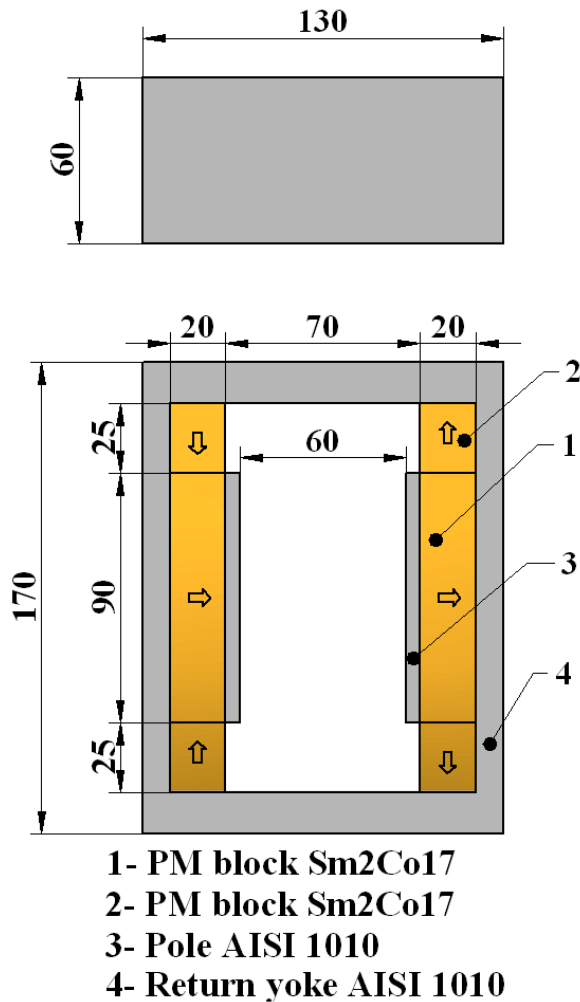
CERN

TE-MSC-MNC

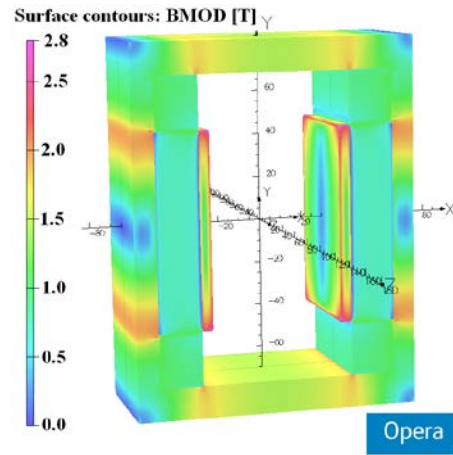
Magnet design

Layout of the dipole magnet

(arrows indicate the direction of magnetization)

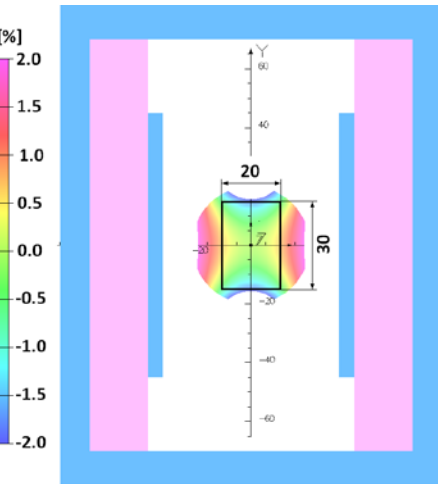


Opera 3D model
with surface field distribution

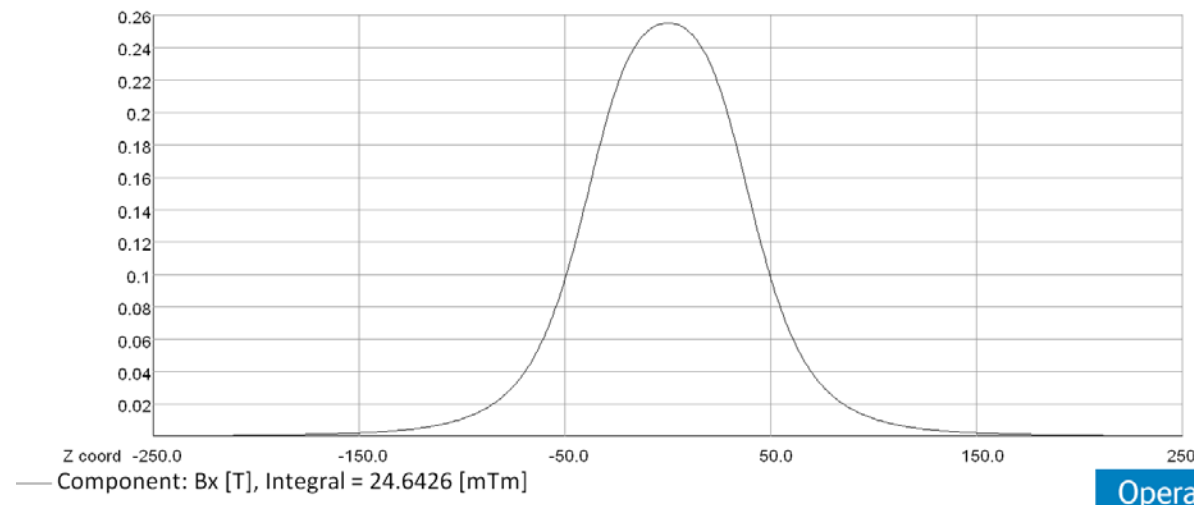


Integrated horizontal field homogeneity
inside the GFR X×Y = 20 mm × 30 mm:

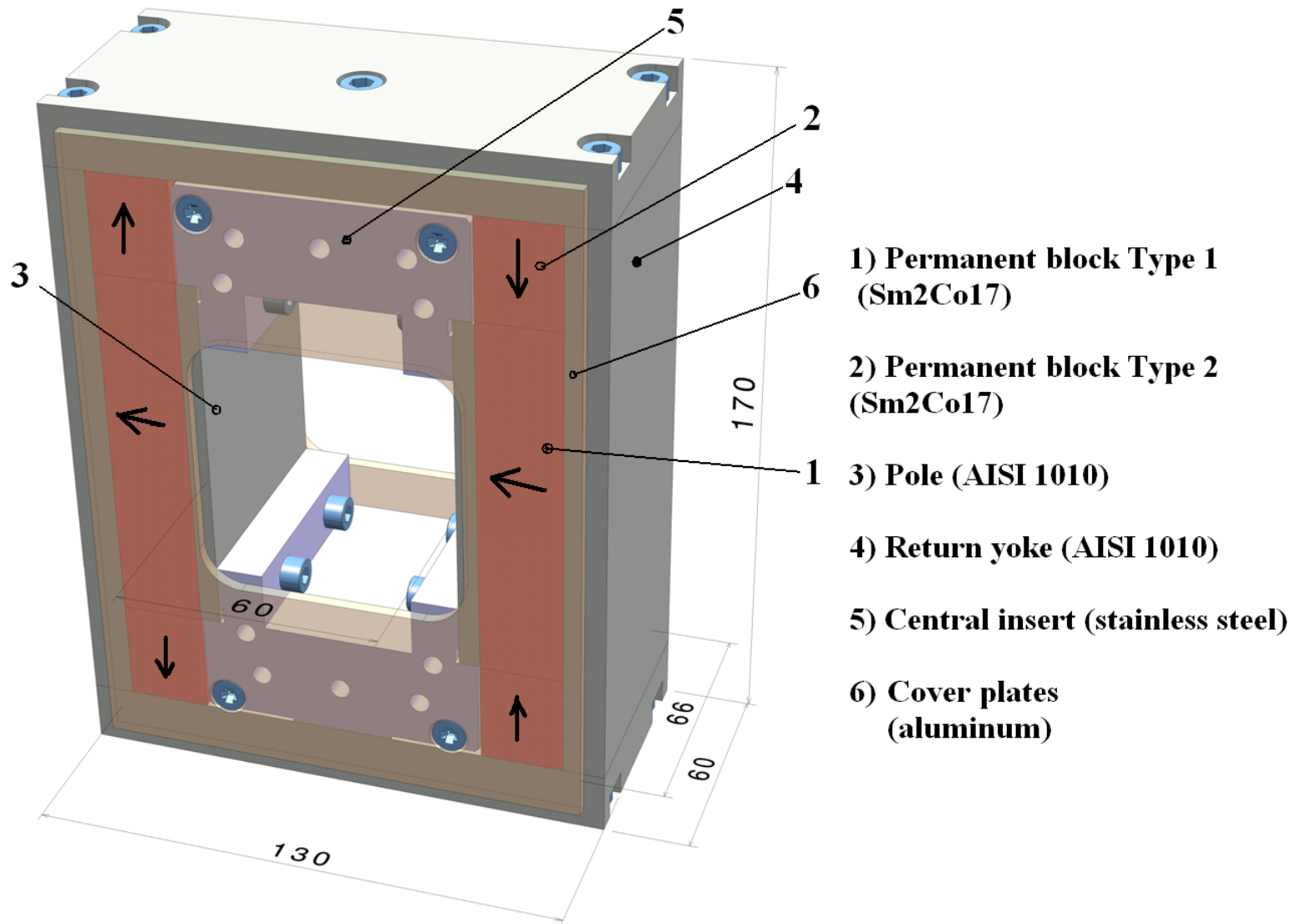
$$\Delta[B_{xdz}/B_x(0,0,z)dz] [\%]$$



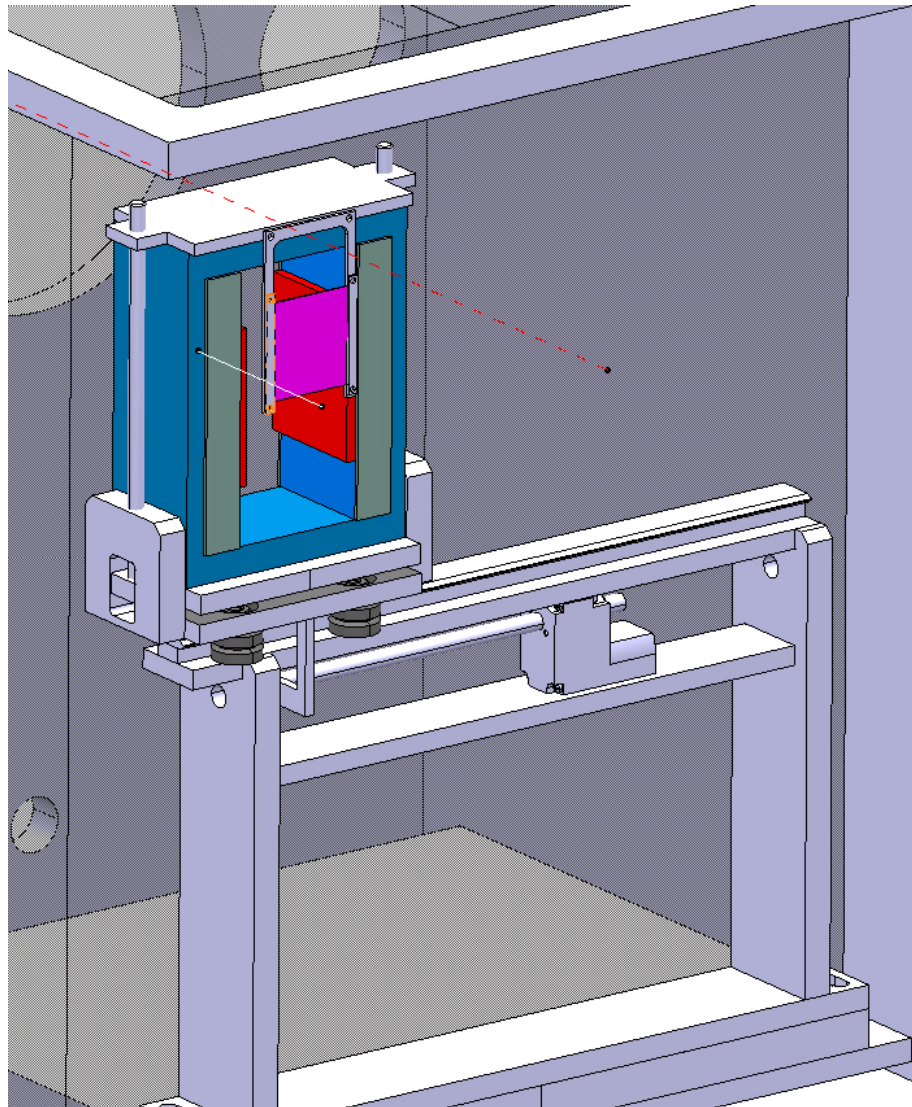
Horizontal field distribution along z-axis at X=Y=0 mm
 $B_x(0,0,z)dz = 24.6 \times 10^{-3} [\text{T} \cdot \text{m}]$



Mechanical structure



Permanent magnet with retractable device



BLUE ... magnet yoke

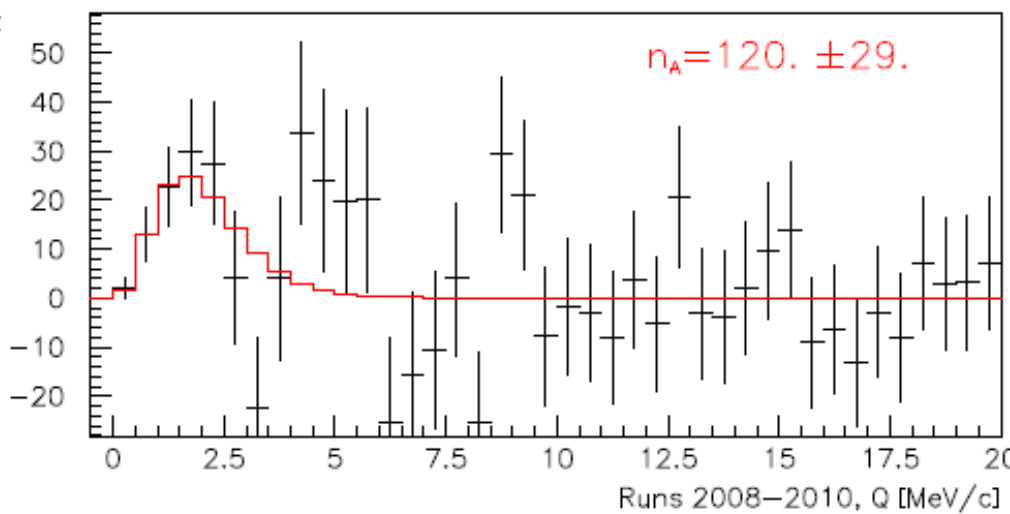
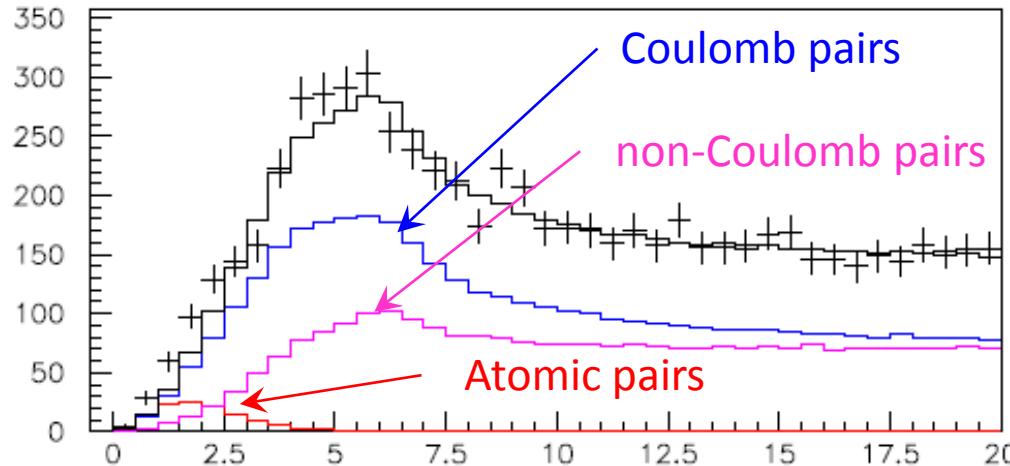
GREY ... magnet poles

RED ... magnet shimming

PURPLE ... Pt foil

I Status of π^+K^- -atoms

A. Benelli, V. Yazkov

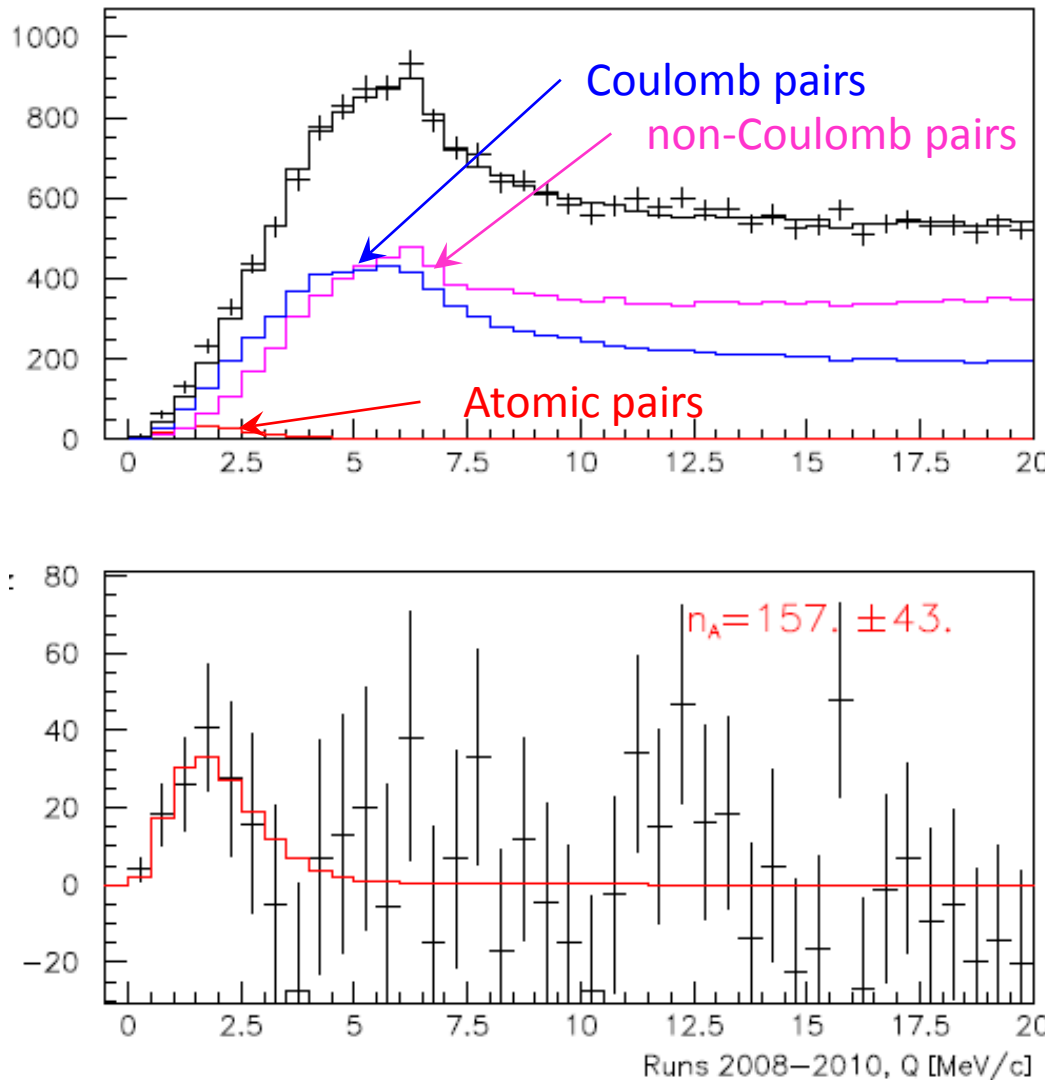


Run 2008-2010, statistics with low and medium background ($\frac{2}{3}$ of all statistics). Point-like production of all particles. The e^+e^- background was not subtracted.

Q – relative momentum in the πK c.m.s.

II Status of π^+K^- -atoms

A. Benelli, V. Yazkov

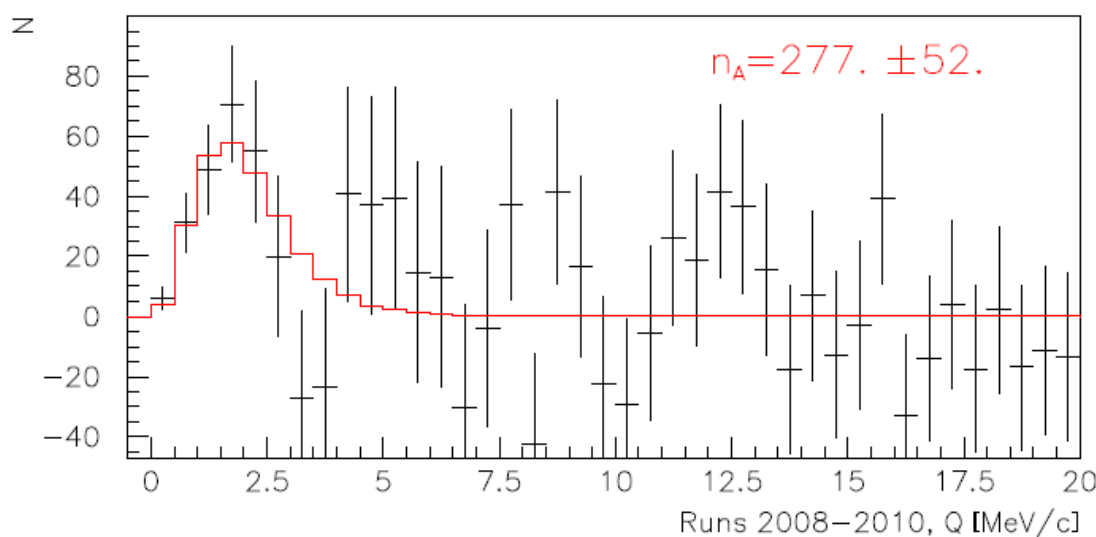
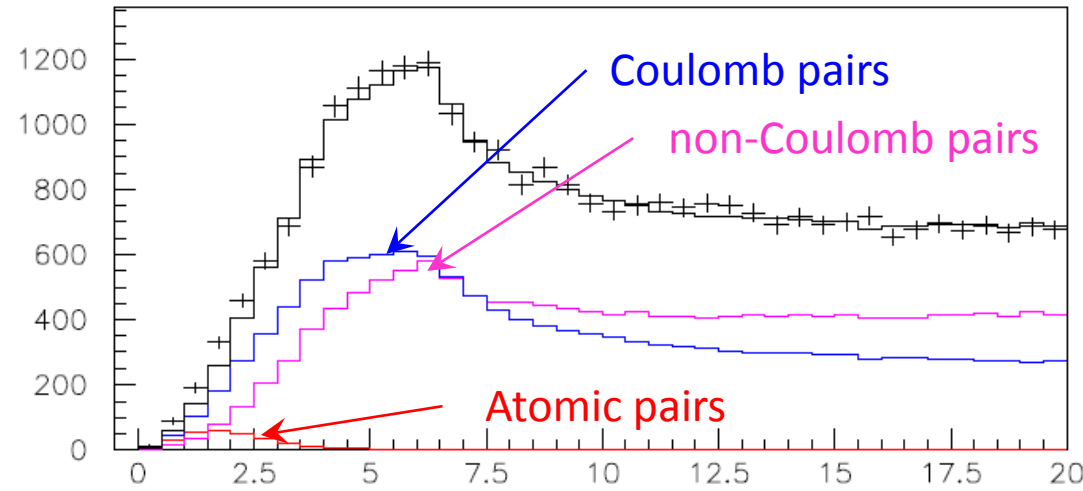


Run 2008-2010, statistics with low and medium background ($\frac{2}{3}$ of all statistics). Point-like production of all particles. The e^+e^- background was not subtracted.

Q – relative momentum in the πK c.m.s.

III. The status of π^-K^+ and π^+K^- atoms

A. Benelli, V. Yazkov

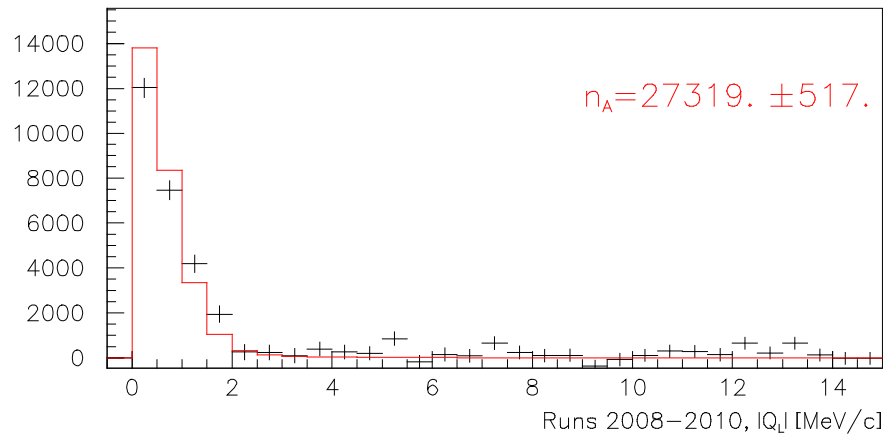
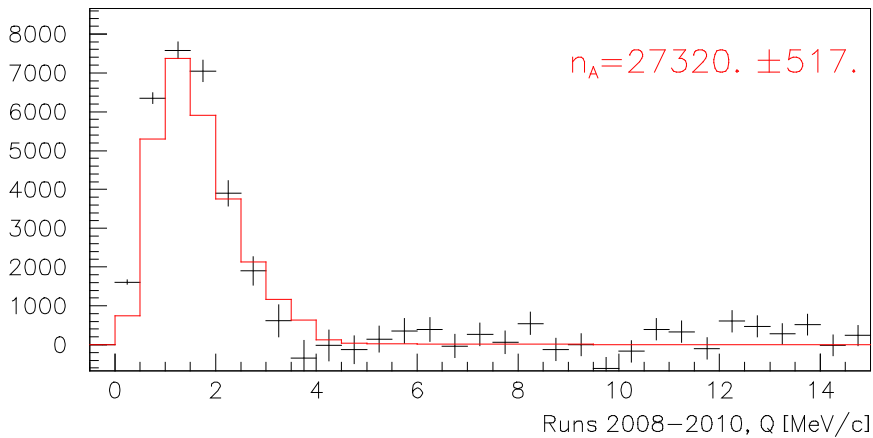
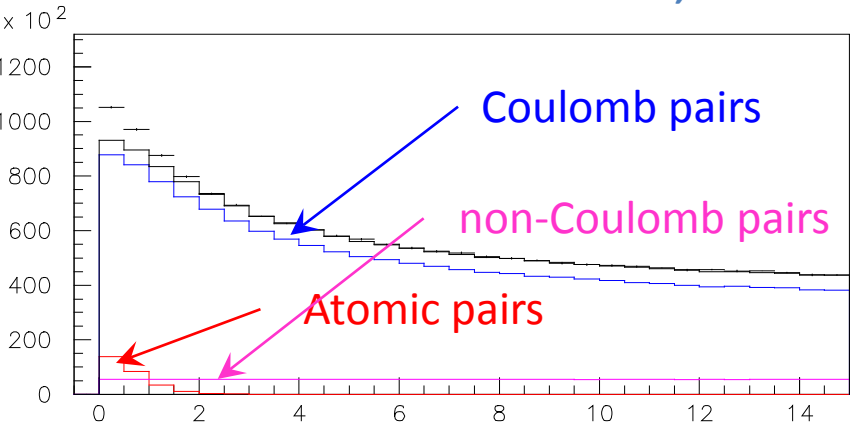
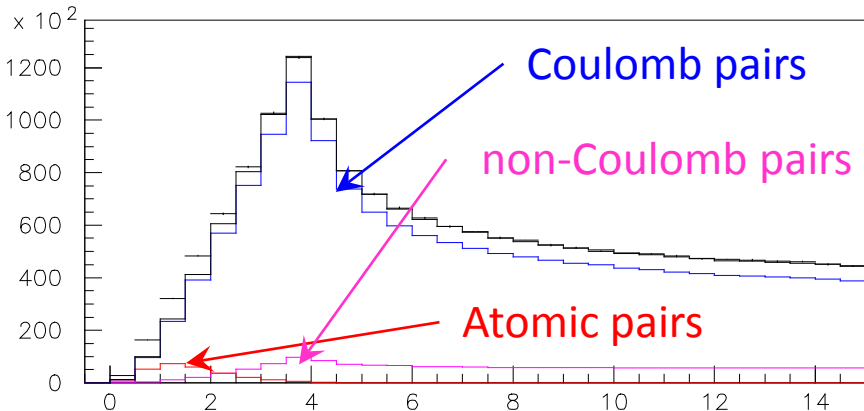


Run 2008-2010,
statistics with low
and medium
background ($\frac{2}{3}$ of all
statistics). Point-like
production of all
particles. The e^+e^-
background was not
subtracted.

Q – relative
momentum in
the πK c.m.s.

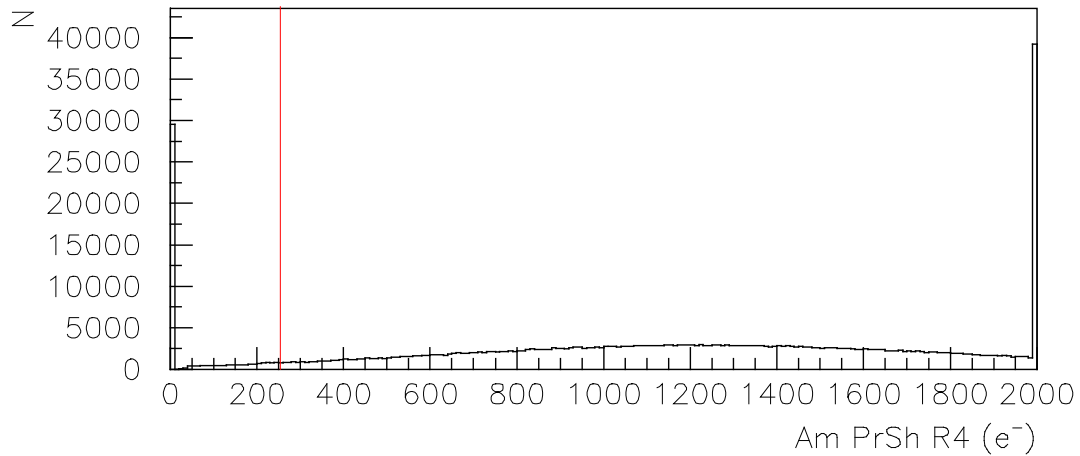
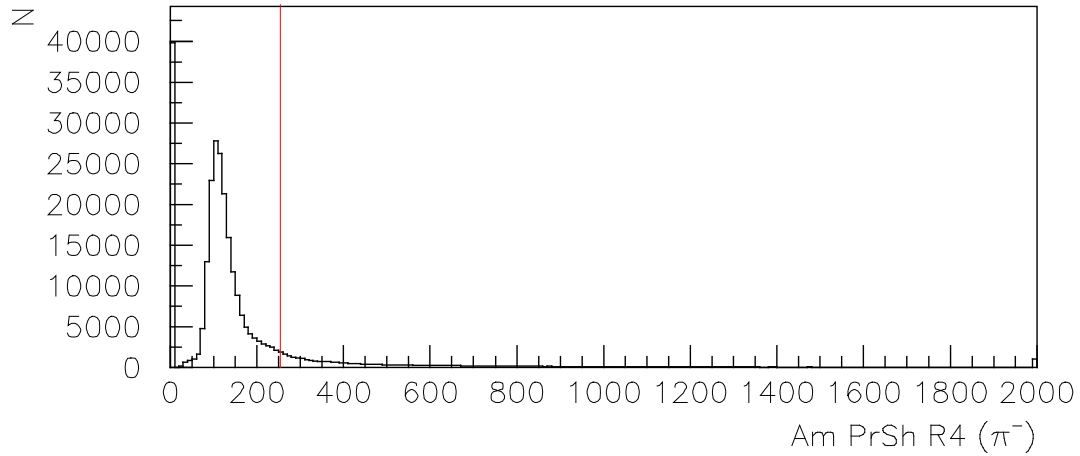
IV Status $\pi^+\pi^-$ -atoms

A. Benelli, V. Yazkov

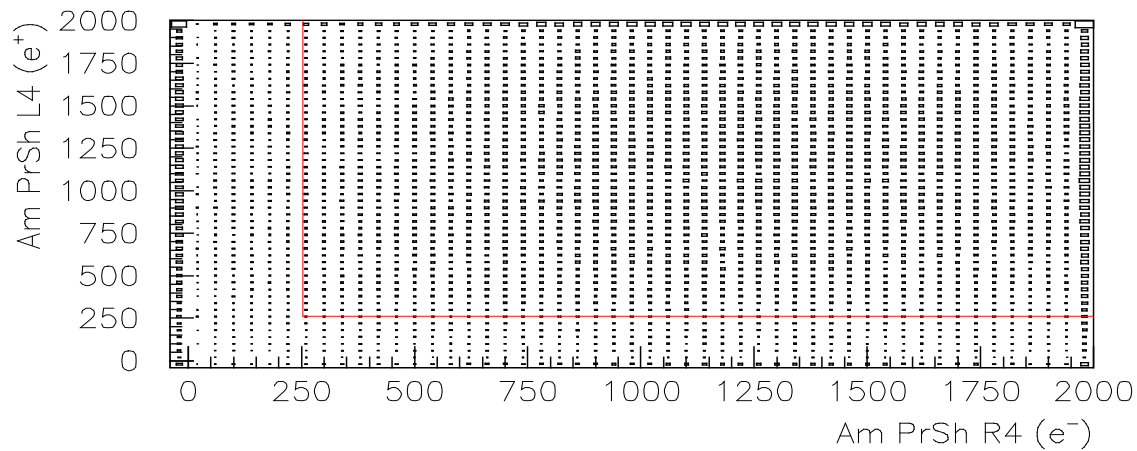
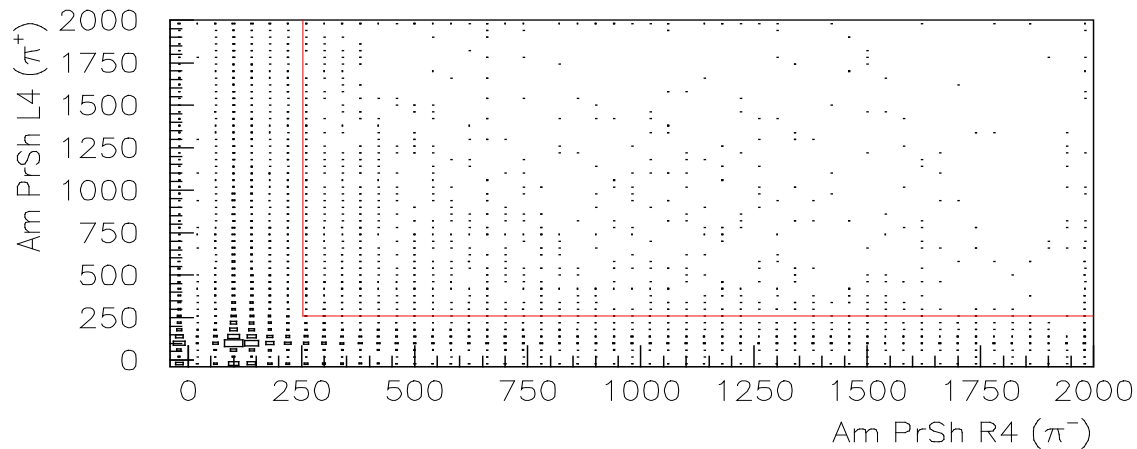


Run 2008-2010, statistics with low and medium background ($\frac{2}{3}$ of all statistics). Point-like production of all particles. The e^+e^- background was not subtracted.

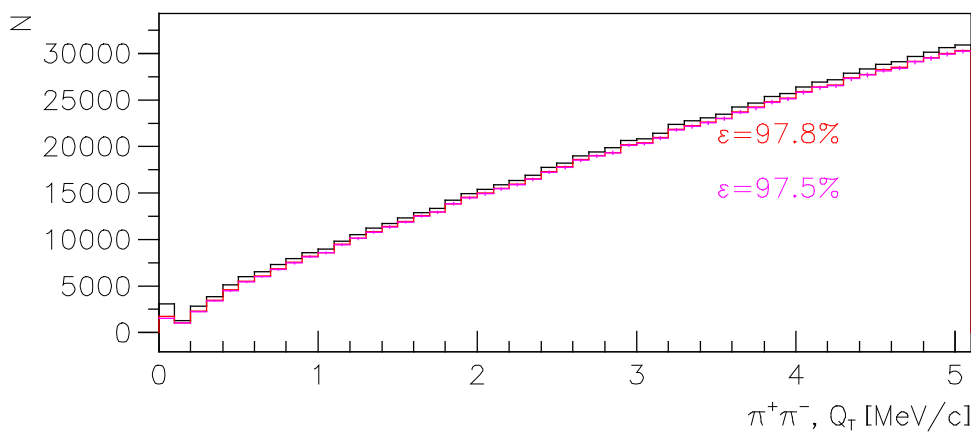
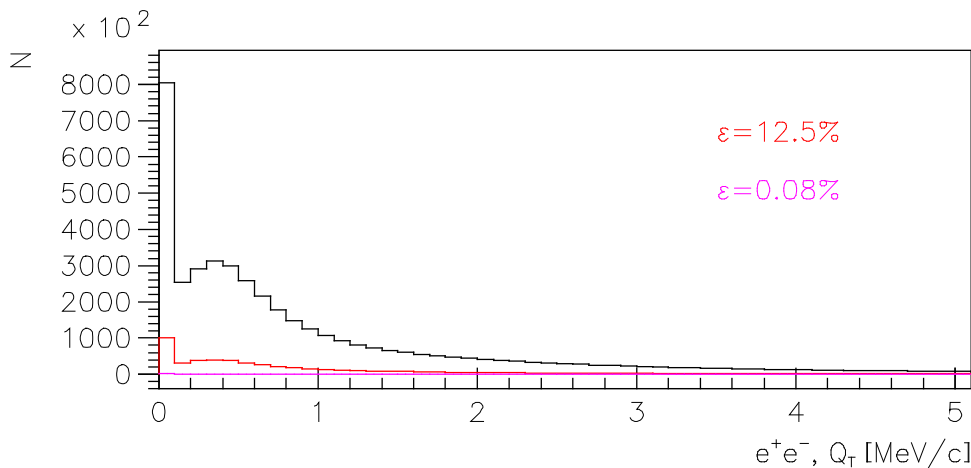
Amplitude distributions for one slab of preshower detector for pions (upper) and electrons (lower). Red line presents criterion for electrons.



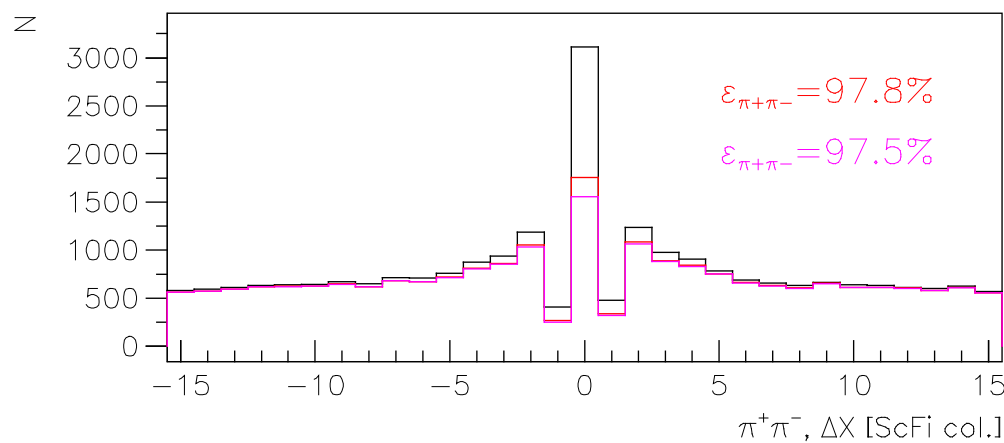
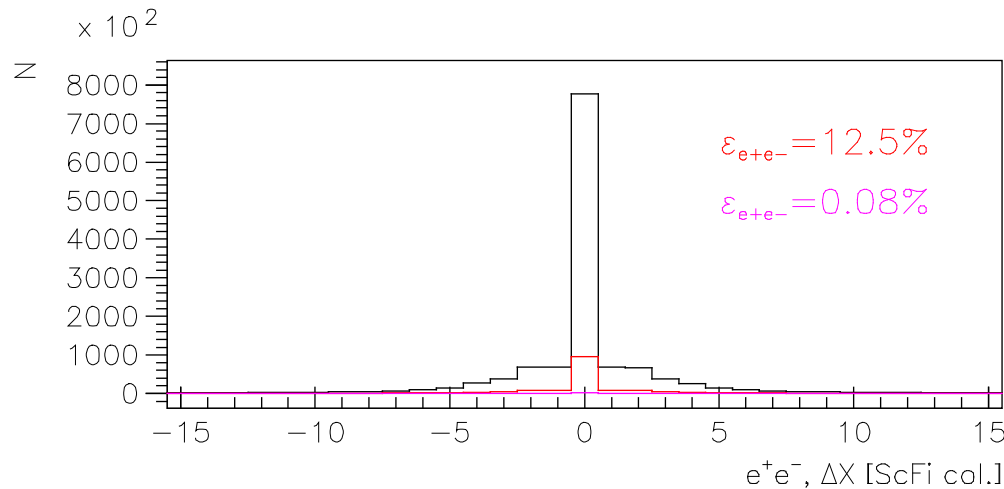
Amplitude distributions for one slab of right arm of preshower
(X-projection) versus amplitude in left arm (Y-projection). Red
line
presents criterion for e+e- pairs.



Transverse momentum distributions for e+e- (upper) and pi+pi- (lower).
All events are in black, events after amplitude criterion are in red
and events after subtraction of weighted electron-like pairs are in magenta.



Coordinated difference at X-plane of ScFi detector distributions for e+e- (upper) and pi+pi- (lower). All events are in black, events after amplitude criterion are in red and events after subtraction of weighted electron-like pairs are in magenta.



$\pi^+\pi^-$ data

Statistics for measurement of $|a_0 - a_2|$ scattering length difference and expected precision

Year	n_A	$\delta_{\text{stat}} (\%)$	$\Delta_{\text{syst}} (\%)$	$\delta_{\text{syst}} (\%) \text{ MS}$	$\delta_{\text{tot}} (\%)$
2001-2003	21000	3.1	3.0	2.5	4.3
2008-2010 *	24000	3.0	3.0	2.5	4.3
2001-2003 2008-2010	45000	2.1	3.0 (2.1)	2.5 (1.25)	3.7 (3.0)

* There is 40% of data with a higher background whose implication is under investigation.

Plan of data analysis of πK and $\pi\pi$ atoms in 2012

1. Run 2008 data analysis without and with e+e- background subtraction:
May 2012
2. Runs 2008, 2009 and 2010 data analysis (all data) without and with e+e- background subtraction:
June 2012.
3. Run 2008, 2009 and 2010 data analysis, taking into account non-pointlike π - and K - mesons production:
October 2012.

Published results on $\pi\pi$ atom: lifetime & scattering length

DIRAC data	τ_{1s} ($10^{-15}s$)					$ a_0 - a_2 $					Reference				
	value	stat	syst	theo*	tot	value	stat	syst	theo*	tot					
2001	2.91	+0.45	+0.19	[+0.49]	0.264	+0.017	+0.022	[+0.033]	PL B 619 (2005) 50	-0.38	-0.49	-0.62	-0.020	-0.009	-0.020
2001-03	3.15	+0.20	+0.20	[+0.28]	0.2533	+0.0078	+0.0072	[+0.0106]	PL B 704 (2011) 24	-0.19	-0.18	-0.26	-0.0080	-0.0077	-0.0111

* theoretical uncertainty included in systematic error

NA48	K-decay	$a_0 - a_2$					Reference
		value	stat	syst	theo	tot	
2009	$K_{3\pi}$	$0.2571 \pm 0.0048 \pm 0.0029$			0.0088		EPJ C64 (2009) 589
2010	$K_{e4} \& K_{3\pi}$	$0.2639 \pm 0.0020 \pm 0.0015$					EPJ C70 (2010) 635

DIRAC prospect at CERN SPS

**Yield of dimeson atoms per one proton-Ni interaction,
detectable by DIRAC upgrade setup at $\Theta_L=5.7^\circ$**

	24 GeV			450 GeV		
E_p	$A_{2\pi}$	$A_{K^+\pi^-}$	$A_{\pi^+K^-}$	$A_{2\pi}$	$A_{K^+\pi^-}$	$A_{\pi^+K^-}$
W_A	$1.1 \cdot 10^{-9}$	$0.52 \cdot 10^{-10}$	$0.29 \cdot 10^{-10}$	$0.13 \cdot 10^{-7}$	$0.10 \cdot 10^{-8}$	$0.71 \cdot 10^{-9}$
W_A^N	1.	1.	1.	12.	19.	24.
W_A/W_π	$3.4 \cdot 10^{-8}$	$16 \cdot 10^{-10}$	$9 \cdot 10^{-10}$	$1.3 \cdot 10^{-7}$	$1 \cdot 10^{-8}$	$7.1 \cdot 10^{-9}$
W_A^N/W_π^N	1.	1.	1.	3.8	6.2	8.
	A multiplier due to different spill duration ~4					
Total gain	1.	1.	1.	15.	25.	32.

Thank you for your attention

Values for energy shifts and lifetimes of $\pi^+\pi^-$ atom

[J. Schweizer, PL B587 (2004) 33]

J. Schacher

(n, ℓ)	ΔE_{nl}^{em} [eV]	ΔE_{nl}^{vac} [eV]	ΔE_{nl}^{str} [eV] ^{*)}	τ_{nl} [10^{-15} s]
(1, 0)	-0.065	-0.942	-3.8 ± 0.1	2.9 ± 0.1
(2, 0)	-0.012	-0.111	-0.47 ± 0.01	23.3 ± 0.7
(2, 1)	-0.004	-0.004	$\approx -1 \square 10^{-6}$	$\approx 1.2 \square 10^4$

→ $\Delta E_{2s-2p} = \Delta E_{20}^{str} + \Delta E_{20}^{em} - \Delta E_{21}^{em} + \Delta E_{20}^{vac} - \Delta E_{21}^{vac} = -0.59 \pm 0.01$ eV

$$\begin{cases} \langle nlm | V_{op} | n'l'm' \rangle \neq 0 & \Rightarrow \text{ Stark mixing} \\ \rightarrow \text{selection rules: } \Delta n = 0, \Delta l = \pm 1, \Delta m = 0 \end{cases}$$

*) $\Delta E_{n0}^{str} \sim A_n(2a_0 + a_2)$

Observation of long-lived $\pi^+\pi^-$ atoms

...opens future possibility to measure the energy splitting $\Delta E(ns-np)$.

$A_{2\pi}$ decay dominated by the annihilation process: $\rightarrow \pi^+ + \pi^- \rightarrow \pi^0 + \pi^0$

$A_{2\pi}$ lifetime depends on the $\pi\pi$ scattering length difference $|a_0 - a_2|$ $\rightarrow \frac{1}{\tau} \approx W_{\pi^0\pi^0} = R |a_0 - a_2|^2$

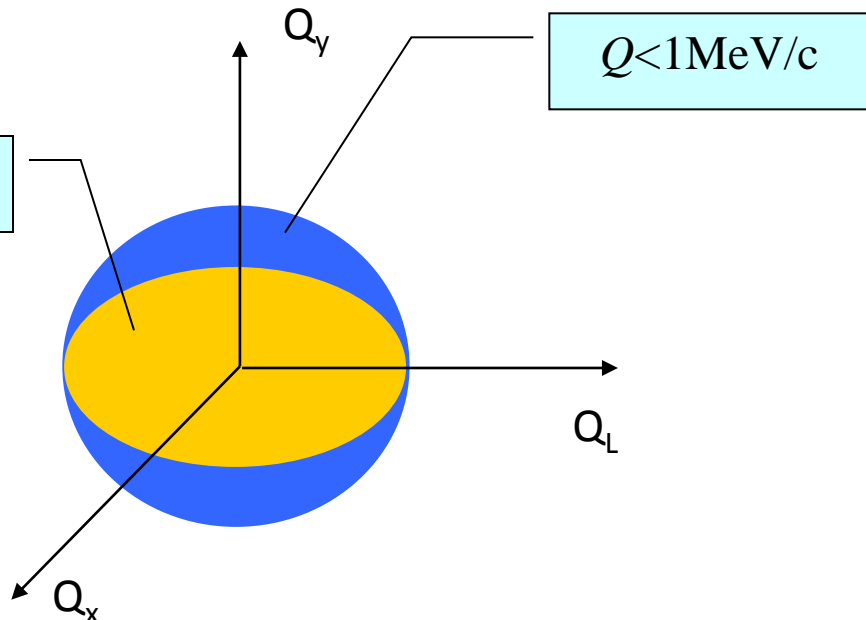
Energy shift contributions $\rightarrow \Delta E_{nl} = \Delta E_{nl}^{em} + \Delta E_{nl}^{vac} + \Delta E_{nl}^{str}$

Strong interaction contribution $\rightarrow \Delta E_{n0}^{str} = A_n (2a_0 + a_2)$

$$\Delta E^{2s-2p} = \Delta E_{20}^{str} + \Delta E_{20}^{em} - \Delta E_{21}^{em} + \Delta E_{20}^{vac} - \Delta E_{21}^{vac} = -0.59 \pm 0.01 eV$$

Simulation of long-lived $A_{2\pi}$ observation

Q and F for Be



$$Q = \sqrt{Q_X^2 + Q_Y^2 + Q_L^2}$$

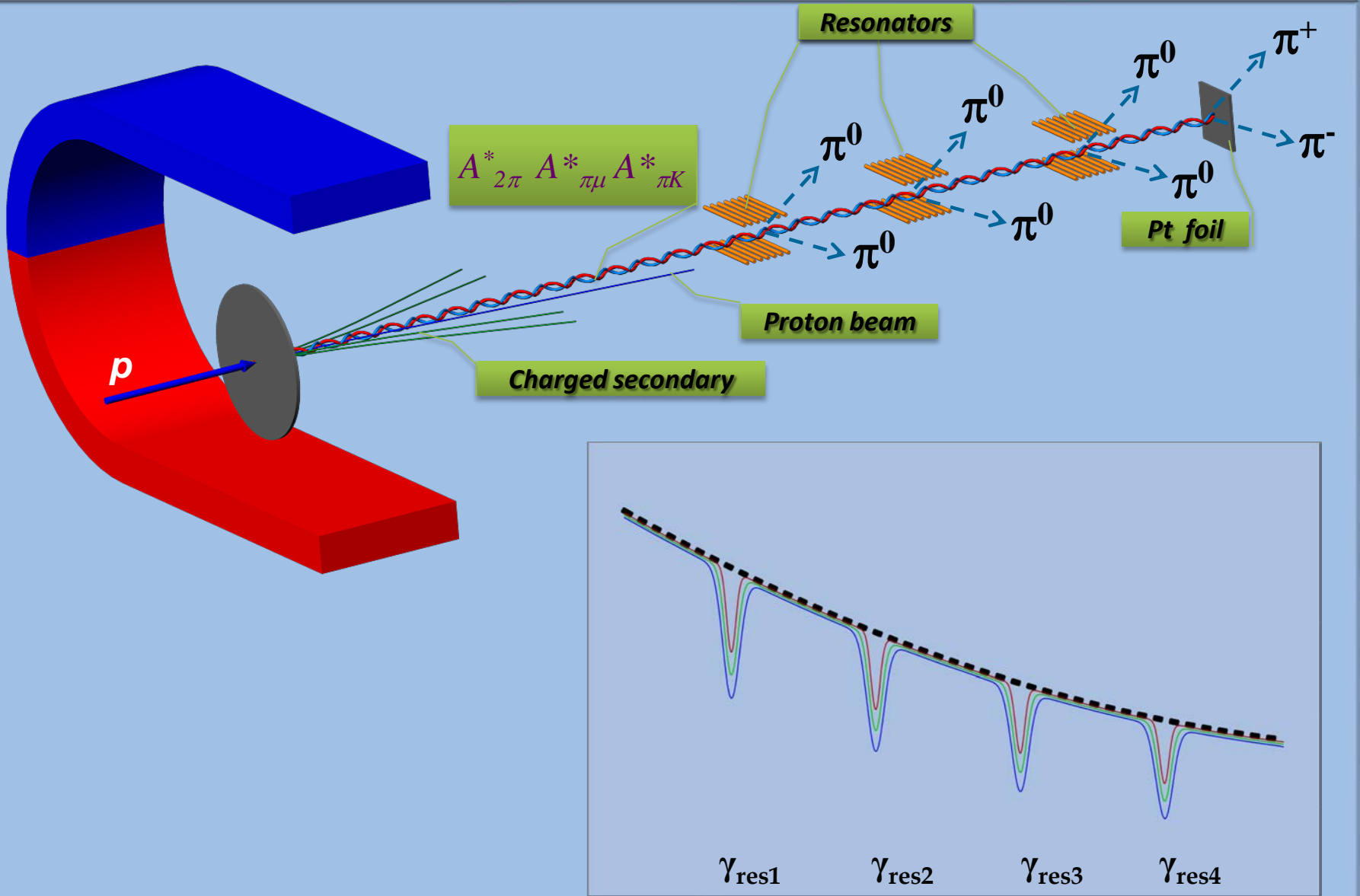
$$F = \sqrt{\frac{Q_X^2}{\sigma_{Q_X}^2} + \frac{Q_Y^2}{\sigma_{Q_Y}^2} + \frac{Q_L^2}{\sigma_{Q_L}^2}}$$

$$\begin{cases} \sigma_{Q_X} = 0.5 MeV / c \\ \sigma_{Q_Y} = 0.32 MeV / c \\ \sigma_{Q_L} = 0.56 MeV / c \end{cases}$$

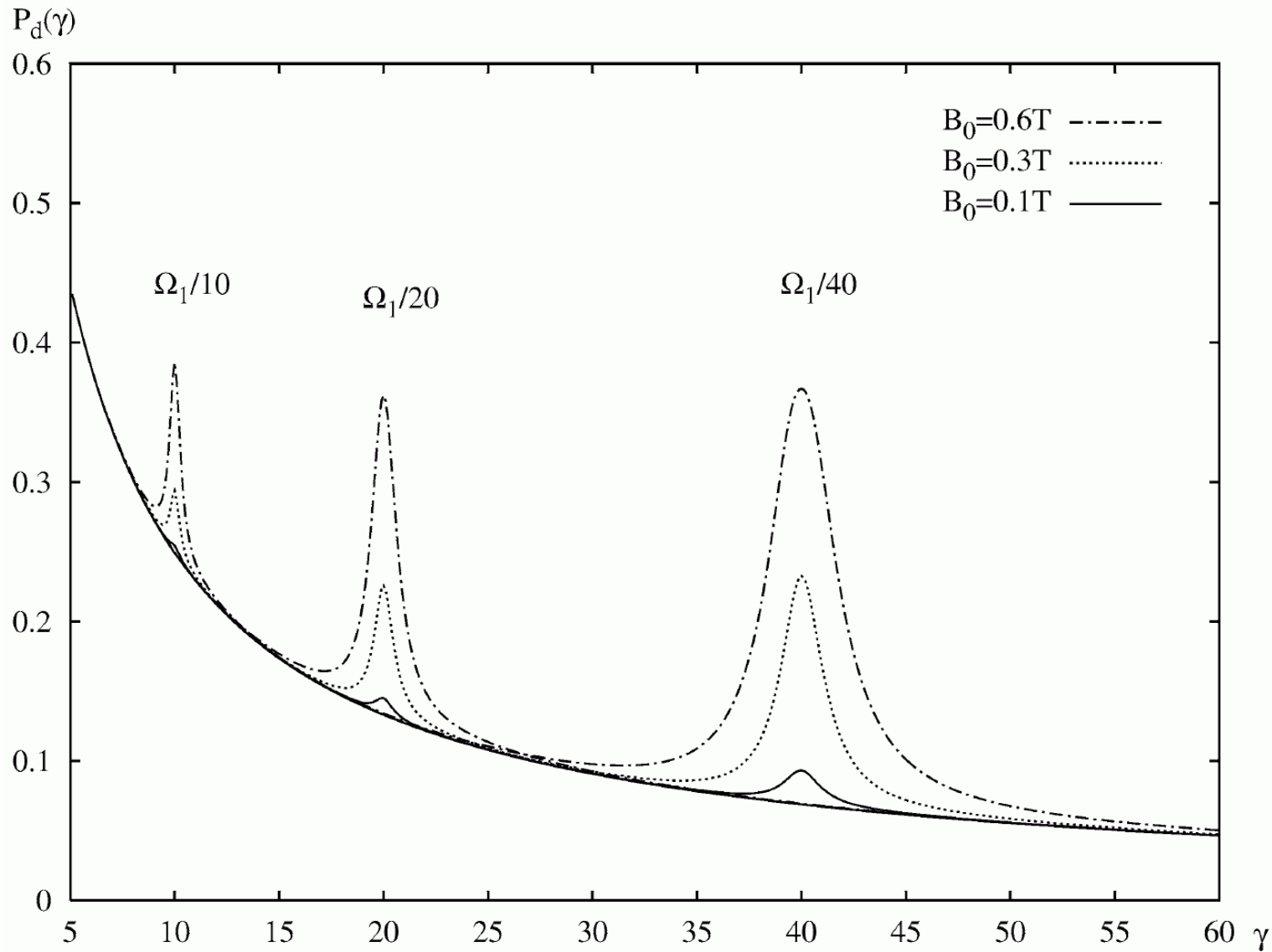
Main parameters

Magnet Type	Permanent Magnet Dipole		
Quantity	1+1(spare)		
Magnet Height Width Length	170 mm	130 mm	66 mm
Magnet mass	8.6 kg		
Full horizontal aperture	60 mm		
Good Field Region(GFR) Horizontal Vertical	20 mm	30 mm	
Magnetic field characteristics			
Nominal integrated horizontal field $\int B_{x(0,0,Z)} dz$	24.6	10^{-3}	T m
Horizontal field in magnet center $B_{x(0,0,0)}$	0.255 T		
Magnetic length $\int B_{x(0,0,Z)} dz / B_{x(0,0,0)}$	96.5 mm		
Integrated field homogeneity inside GFR $\Delta \int B_x dz / \int B_{x(0,0,Z)} dz$	< 2%		
Components			
Permanent magnet blocks	Sm2Co17, "Recoma 30S" or equivalent		
Pole and Return Yoke	Low carbon steel: AISI 1010		
Central inserts	Stainless steel: 316L+N		
Cover plates	Aluminum: EN-AW-6082		

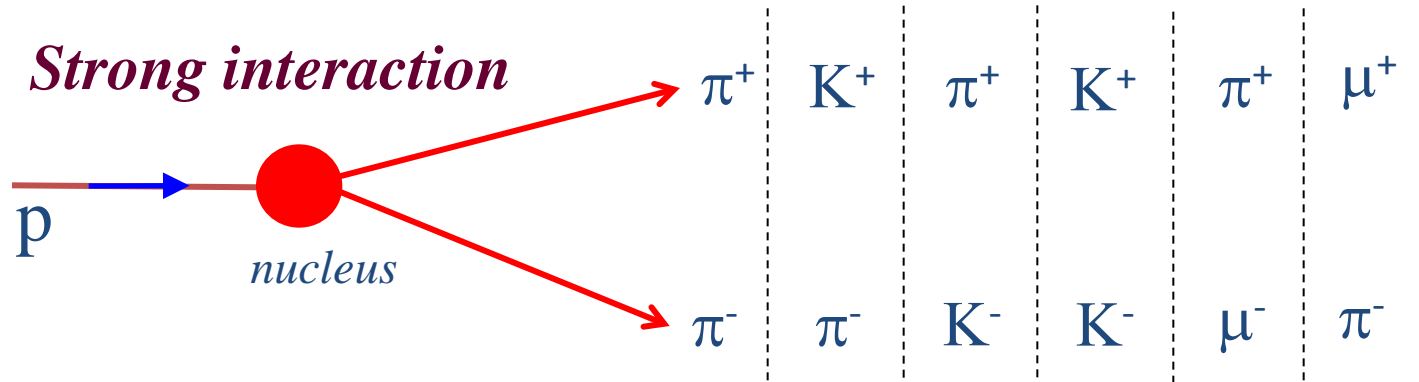
Resonant method



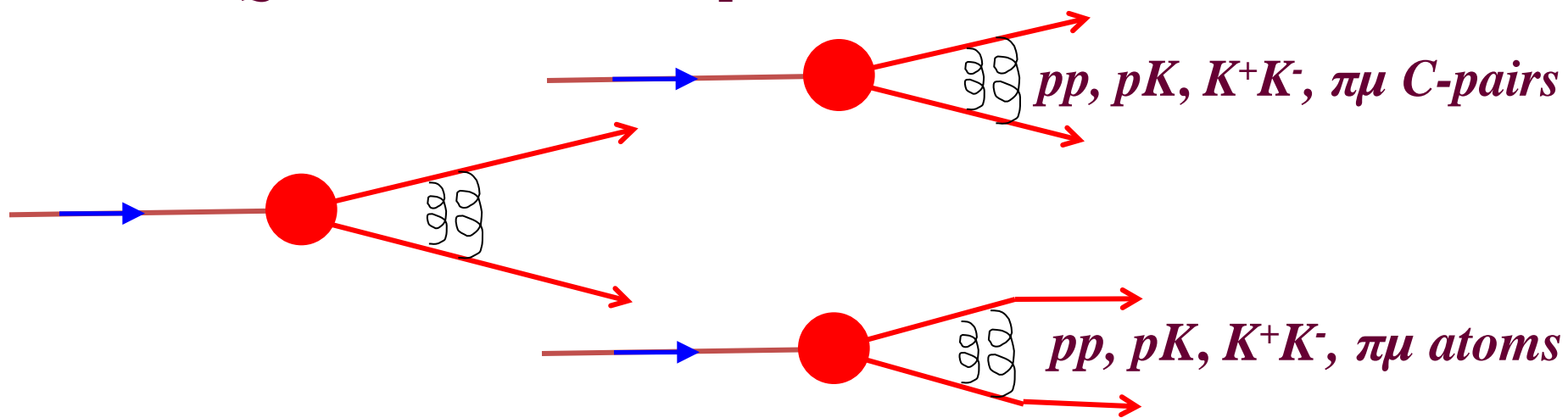
Resonant enhancement



Coulomb pairs and atoms

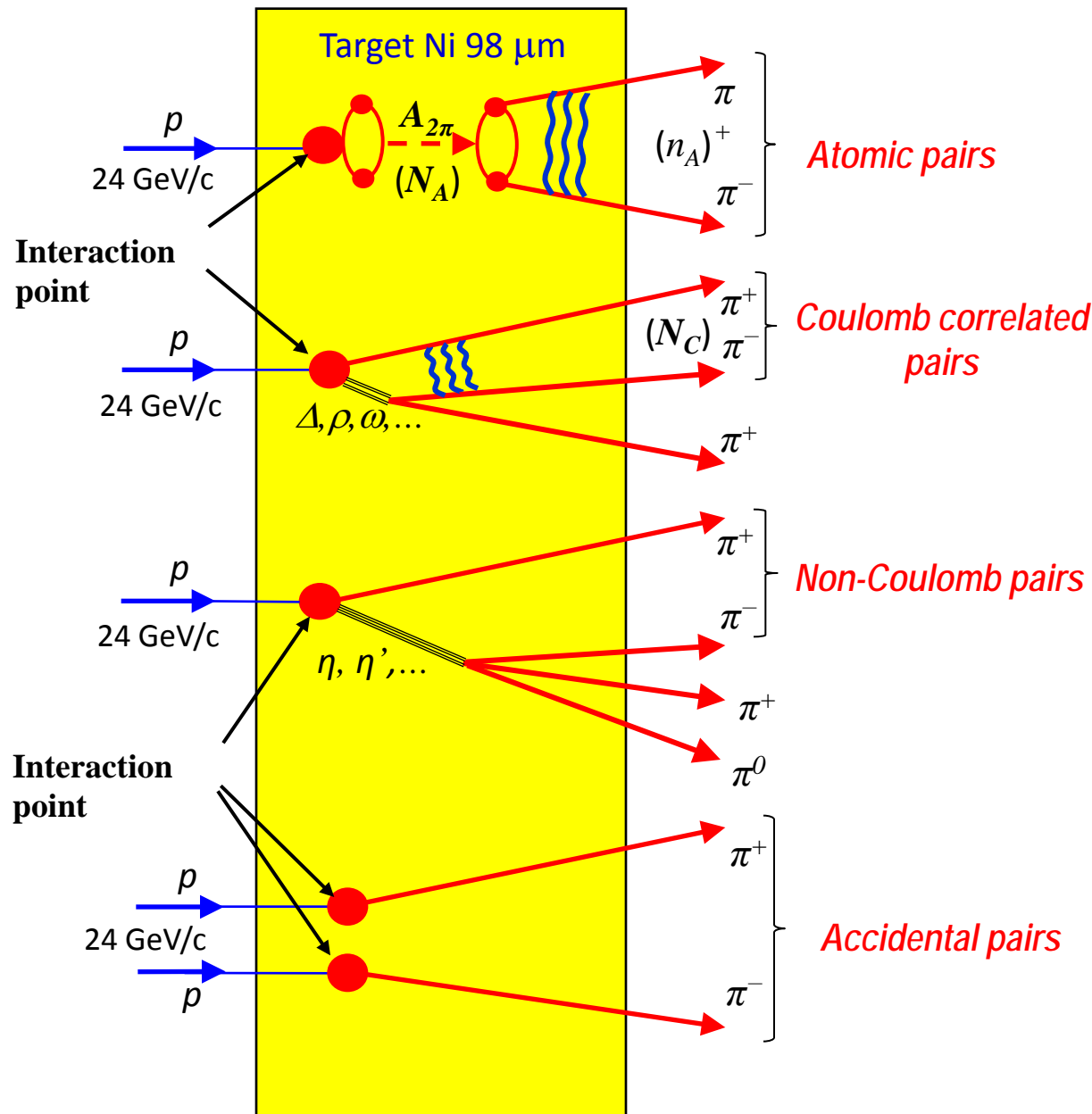


For small Q there are Coulomb pairs :

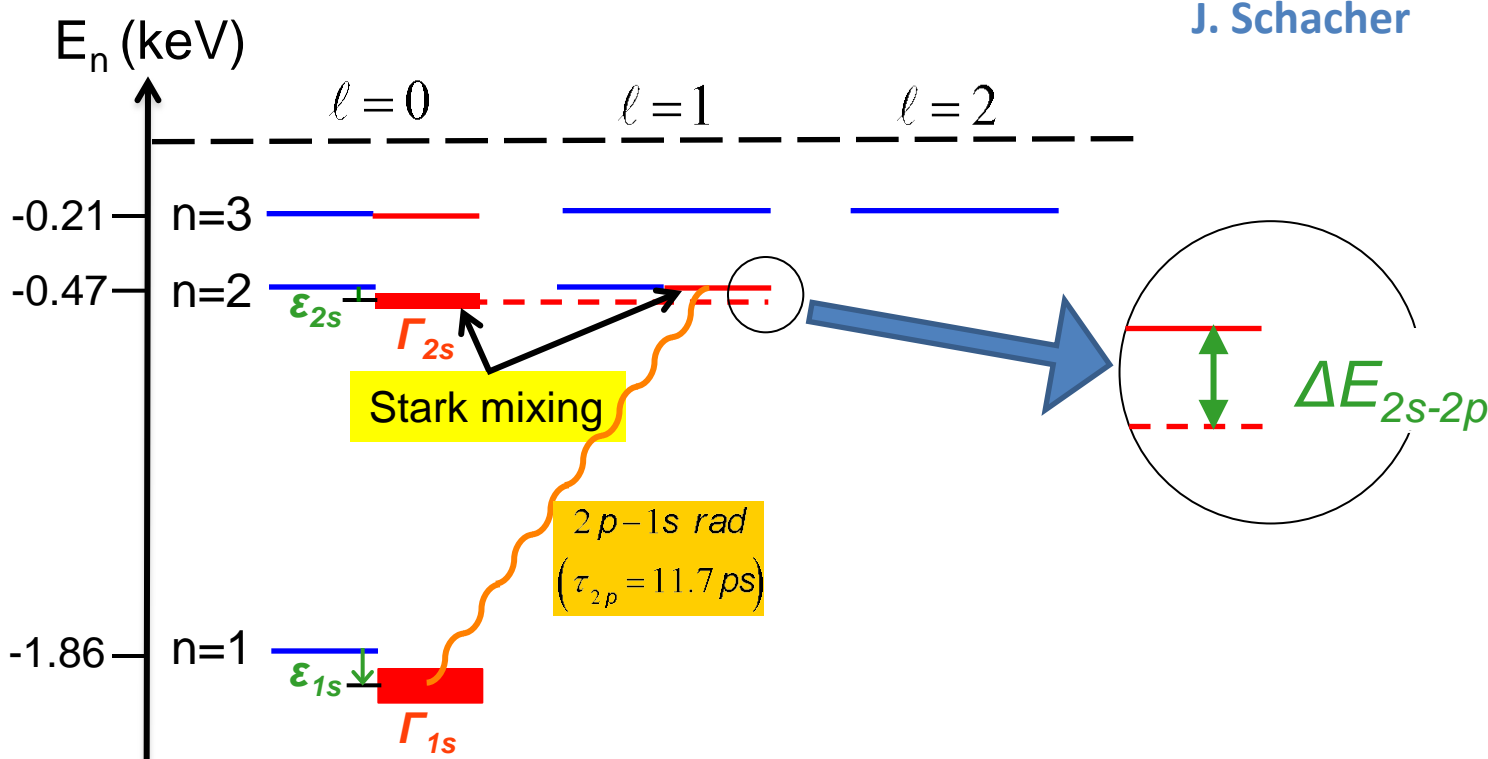


The production yield strongly increases for smaller Q

Method of $A_{2\pi}$ observation and measurement



$A_{2\pi}$ level scheme and $2s - 2p$ energy splitting



$$\rightarrow \underline{\varepsilon_{nl}} \equiv \Delta E_{nl} = \sum_i \Delta E_{nl}^i : \varepsilon_{1s} = -4.807 \text{ eV}; \varepsilon_{2s} = -0.593 \text{ eV}; \varepsilon_{2p} = -0.008 \text{ eV}$$

$$\Rightarrow \underline{\Delta E_{2s-2p}} = \varepsilon_{2s} - \varepsilon_{2p} = -0.585 \text{ eV}$$

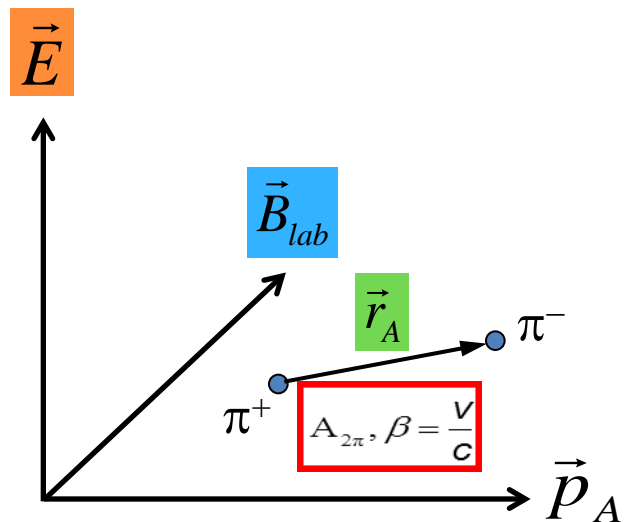
$\left\{ \begin{array}{l} \text{2s level shifted below 2p level} \\ \text{by } \approx 0.6 \text{ eV "Lamb" shift} \end{array} \right.$

$$\rightarrow \underline{\Gamma_n} \equiv \Gamma_n(\pi^0 \pi^0) = \tau_n^{-1} : \tau_{1s} = 2.9 \text{ fs}; \tau_{2s} = 8 \cdot \tau_{1s} = 23.2 \text{ fs}$$

Lamb shift measurement with external magnetic field

See: L. Nemenov, V. Ovsiannikov, Physics Letters B 514 (2001) 247.

Impact on atomic beam by
external magnetic field \vec{B}_{lab} and Lorentz factor γ



\vec{r}_A relative distance between
 π^+ and π^- in A_{2π} system

\vec{B}_{lab} laboratory magnetic field

\vec{E} ...electric field in A_{2π} system

$$|\vec{E}| = \beta \gamma B_{lab} \approx \gamma B_{lab}$$

H=0.0 T $\xi=1$ $N_A=330 \pm 40$
H=0.1 T $\xi=1$ $N_A=330$ (1-0.7%)

V. Brekhovskikh

ξ	0.4	1	1.6
H=0.4 T	328	317	302
	11	15	13
H=0.6 T	325	304	279
	21	25	23
H=0.8 T	322	290	258
	32	32	32
H=1.0 T	317	276	241
	41	35	38
H=1.2 T	312	263	227
	49	36	46
H=1.4 T	307	251	215
	56	36	46
H=1.6 T	302	241	206
	61	35	48

Δ_{2s-2p} can be measured at H = 1.4 ÷ 1.6 T with 60% precision using low level background events and with 50% precision using low level and medium level background events.

Magnetic Field - 1.0 T

V. Brekhovskikh

Magnetic Field 1.0 T $\xi = 40\%$ 317.273

	2p	3p	4p	5p	6p	7p	8p	Σ
n,%	0.42	0.27	0.15	0.079	0.046	0.025	0.012	1.002
$\tau \cdot 10^{-11}, s$	1.17	3.94	9.05	17.5	29.9	46.8	69.3	177.66
L,cm	5.64	19.02	43.68	84.47	144.32	225.89	334.49	857.50
ξ_n	0.0075	0.0254	0.0603	0.1177	0.2034	0.3231	0.4822	1.2197
$\tau_{eff} \cdot 10^{-11}, s$	1.162	3.656	6.302	6.571	5.011	3.461	2.397	28.561
L_{eff}, cm	5.609	17.647	30.418	31.715	24.188	16.703	11.572	137.85
N_a	0.0714	0.1595	0.1193	0.0701	0.0429	0.0239	0.0116	0.499
N_a^{eff}	0.0710	0.1557	0.1124	0.0624	0.0349	0.0171	0.0070	0.4605

Magnetic Field 1.0 T $\xi = 100\%$ 276.147

	2p	3p	4p	5p	6p	7p	8p	Σ
n,%	0.42	0.27	0.15	0.079	0.046	0.025	0.012	1.002
$\tau \cdot 10^{-11}, s$	1.17	3.94	9.05	17.5	29.9	46.8	69.3	177.66
L,cm	5.64	19.02	43.68	84.47	144.32	225.89	334.49	857.50
ξ_n	0.0188	0.0636	0.1507	0.2943	0.5086	0.8076	1.2056	3.0492
$\tau_{eff} \cdot 10^{-11}, s$	1.122	2.653	2.429	1.535	0.933	0.590	0.395	9.659
L_{eff}, cm	5.416	12.806	11.726	7.412	4.504	2.849	1.907	46.622
N_a	0.0714	0.1595	0.1193	0.0701	0.0429	0.0239	0.0116	0.499
N_a^{eff}	0.0683	0.1369	0.0821	0.0335	0.0118	0.0030	0.0005	0.3362

Magnetic Field 1.0 T $\xi = 160\%$ 240.908

	2p	3p	4p	5p	6p	7p	8p	Σ
n,%	0.42	0.27	0.15	0.079	0.046	0.025	0.012	1.002
$\tau \cdot 10^{-11}, s$	1.17	3.94	9.05	17.5	29.9	46.8	69.3	177.66
L,cm	5.64	19.02	43.68	84.47	144.32	225.89	334.49	857.50
ξ_n	0.0301	0.1017	0.2411	0.4709	0.8137	1.2922	1.9289	4.8788
$\tau_{eff} \cdot 10^{-11}, s$	1.055	1.757	1.135	0.634	0.372	0.233	0.155	5.339
L_{eff}, cm	5.092	8.483	5.476	3.059	1.793	1.122	0.747	25.774
N_a	0.0714	0.1595	0.1193	0.0701	0.0429	0.0239	0.0116	0.499
N_a^{eff}	0.0637	0.1079	0.0458	0.0106	0.0016	0.0001	$3.87 \cdot 10^{-6}$	0.2296

The lifetime of $A_{2\pi}$ in electric field

L. Nemenov, V. Ovsiannikov (P. L. 2001)

$$M = \frac{3F\hbar^2}{\mu_l} \delta_{m,0}, \quad F - \text{strength of electric field in } A_{2\pi} \text{ c.m.s.}$$

$$F = \beta\gamma B_L, \quad B_L \text{ in lab. syst.}$$

→ m must be 0

$$\xi = \frac{2 M}{\Omega_1}, \quad \Omega_1(n = 2) = \frac{E_{2s} - E_{2p}}{\hbar}$$

$$\xi(2s - 2p) = \xi_0 \gamma B_L \quad \xi_0 \sim \frac{1}{E_{2s} - E_{2p}} \quad \xi_n = \frac{\xi_0}{8} n^3 \gamma B_L$$

$$\tau_n^{eff} = \frac{\tau_n}{1 + 120\xi_n^2}$$

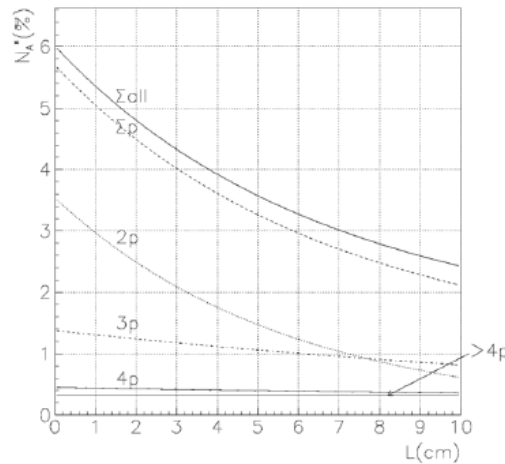
CONCLUSION: the lifetimes for long-lived states can be calculated using only one parameter → $E_{2s} - E_{2p}$.

The probability $W(m=0)$ of $A_{2\pi}$ to have $m=0$ on \vec{F} will be calculated by L. Afanasev. The preliminary value is $W(m=0) \approx 50\%$.

Annihilation of long-lived $A_{2\pi}$

Lifetimes τ from np states and their lab decay lengths λ in for $\gamma = 16$

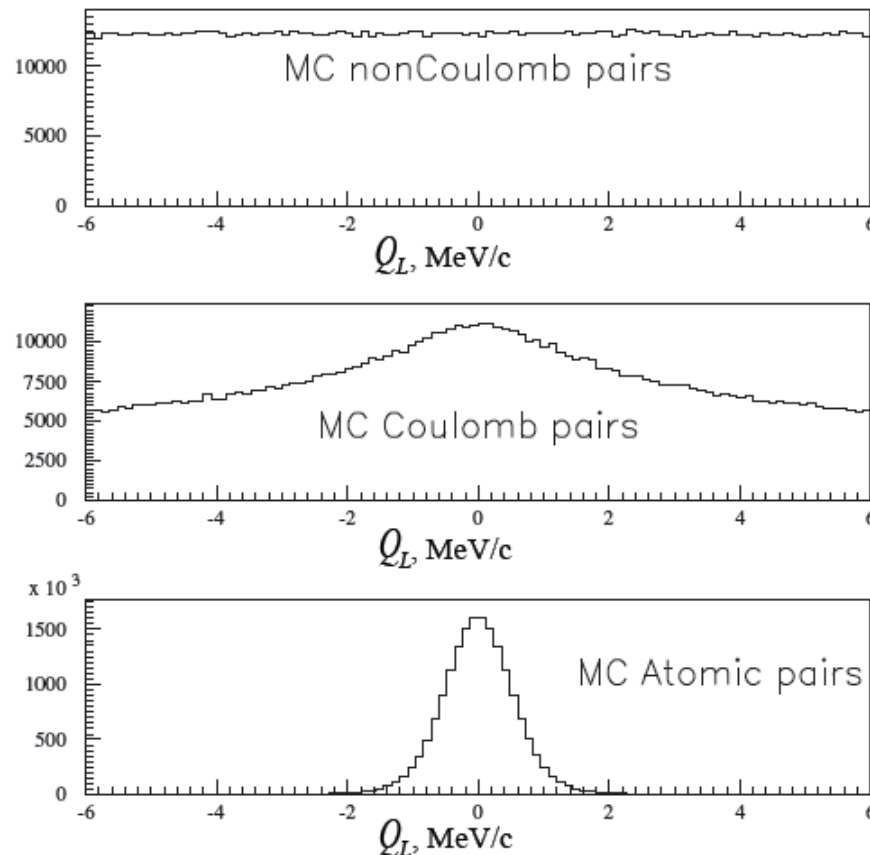
state	$\tau \cdot 10^{11} \text{ s}$	$\lambda [\text{cm}]$
2p	1.17	5.7
3p	3.94	19
4p	9.05	44
5p	17.5	84.5
6p	29.9	144
7p	46.8	226
8p	69.3	335



Part of atoms created in the Be target and then broken up in the Pt foil versus the distance between the target and foil (L) for all metastable states with $n > 1, l > 0$ (Σ all), for sum of np states (Σp) and for some individual p states. The foil thickness is $2 \mu\text{m}$.

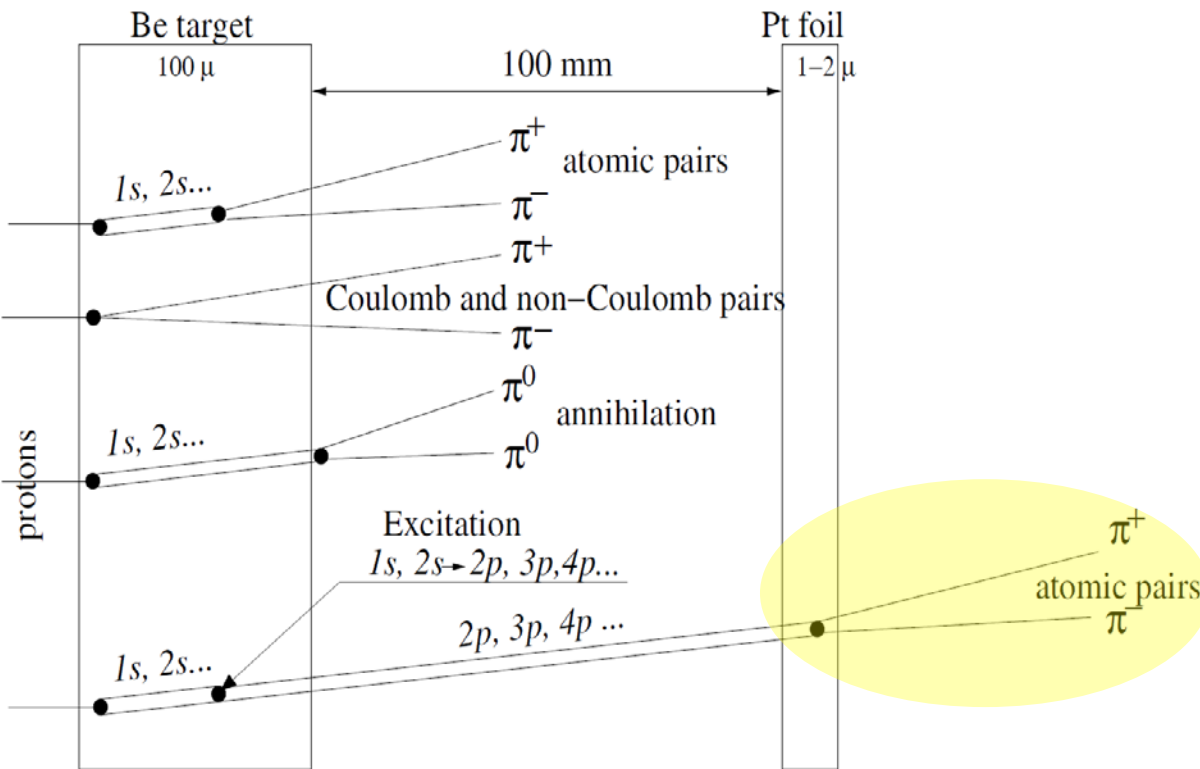
Simulation of $\pi^+\pi^-$ pairs from Beryllium target and "atomic pairs" from Platinum foil

Distributions of reconstructed values of Q_L for non-Coulomb, Coulomb pairs and pairs from metastable atom



Observation method

The $A_{2\pi}$ decay in the p -state is forbidden by angular momentum conservation. So the lifetime of the $A_{2\pi}$ atom in the $2p$ state ($\tau_{2p} = 1.17 \cdot 10^{-11}$ s) is determined by the $2p-1s$ radiative transition with a subsequent annihilation in $1s$ state ($\tau_{1s} = 3 \cdot 10^{-15}$ s): $\pi^+ + \pi^- \rightarrow \pi^0 + \pi^0$



For $p_A = 4.5$ GeV/c
($\gamma = 16.1$)

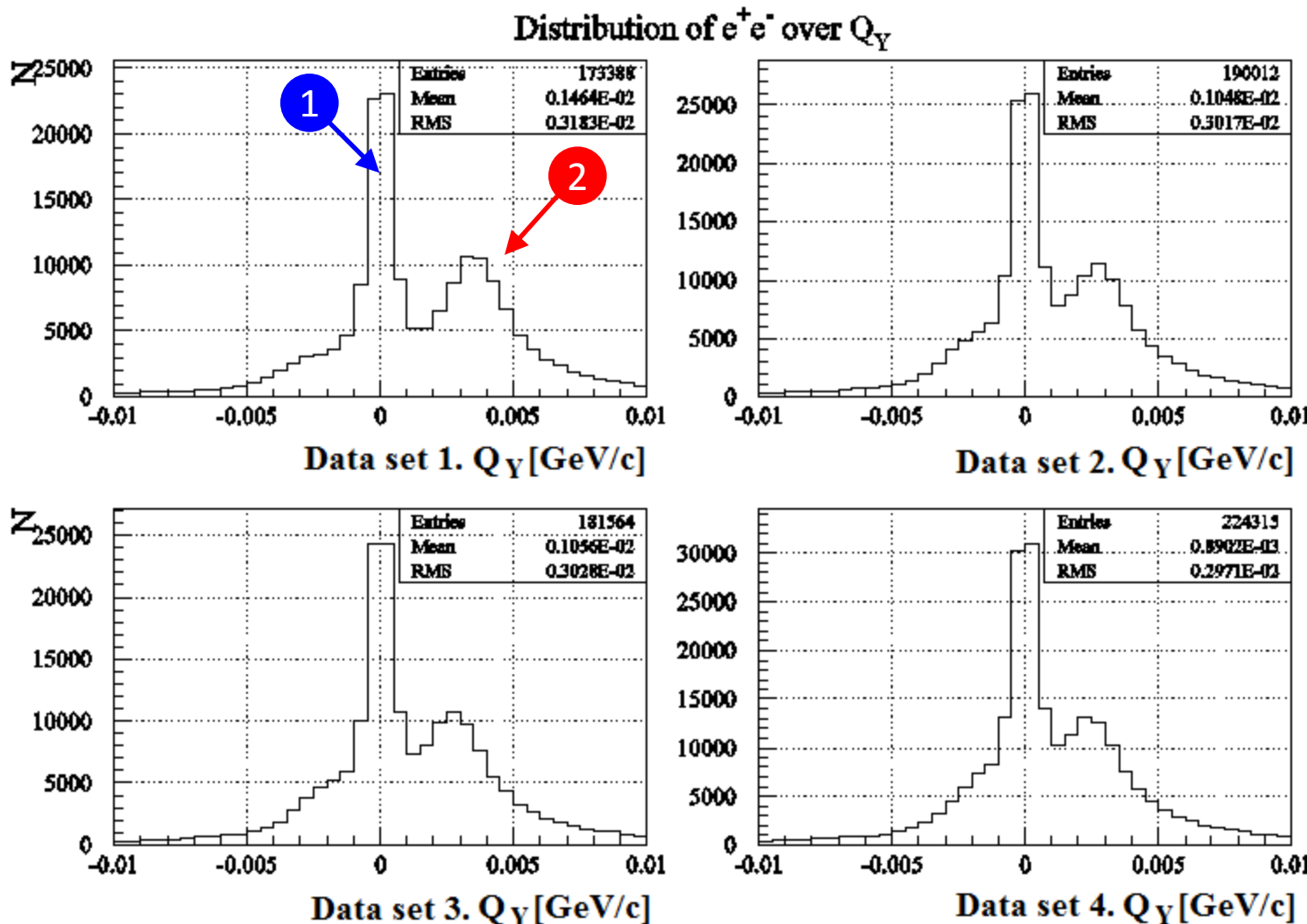
$$\left\{ \begin{array}{ll} \tau_{1s} = 2.9 \cdot 10^{-15} \text{ s}, & \lambda_{1s} = 1.4 \cdot 10^{-3} \text{ cm} \\ \tau_{2s} = 2.3 \times 10^{-14} \text{ s}, & \lambda_{2s} = 1.1 \times 10^{-2} \text{ cm} \\ \tau_{2p} = 1.17 \times 10^{-11} \text{ s}, & \lambda_{2p} = 5.7 \text{ cm}, \lambda_{3p} \approx 19 \text{ cm}, \\ & \lambda_{4p} \approx 43 \text{ cm} \end{array} \right.$$

The lifetime of the np -states is about 10^3 larger than the ns -states, so it is possible to measure the **energy difference of these levels** by exerting an **electric field** (Stark effect) on the atom and tracking the field dependence of the decay probability.

The influence of an **magnetic field** on the $A_{2\pi}$ atom lifetime opens the possibility to measure the **splitting between 2s and 2p levels**.

Shift of Q_Y (June-August) e^+e^- data

F. Takeutchi, V. Yazkov



1

Pairs generated after magnet

2

Pairs generated on Be target
before magnet